



Cite this: *Green Chem.*, 2021, **23**, 8995

## Incorporation of catechyl monomers into lignins: lignification from the non-phenolic end *via* Diels–Alder cycloaddition?†

Daisuke Ando, <sup>‡,a</sup> Fachuang Lu, <sup>a,b</sup> Hoon Kim, <sup>a</sup> Alexis Eugene, <sup>a</sup> Yuki Tobimatsu, <sup>c</sup> Ruben Vanholme, <sup>d,e</sup> Thomas J. Elder, <sup>f</sup> Wout Boerjan <sup>d,e</sup> and John Ralph <sup>\*,a,g,h</sup>

Canonical lignification occurs *via* the coupling of phenolic radicals, in which chain extension can occur only from phenolic ends of growing polymer chains. Radical coupling of catechyl monomers, including caffeyl and 5-hydroxyconiferyl alcohols, gives rise to benzodioxane units in the polymer. Anticipating that a catechol could oxidize to its *o*-benzoquinone analog under the dehydrogenative (oxidative) conditions of lignification, we examined the possibility that an *o*-benzoquinone, as the diene component, could also incorporate into lignin *via* another mechanism, the Diels–Alder cycloaddition reaction. The *o*-benzoquinone derived from methyl 5-hydroxyvanillate and 4-*O*-methylconiferyl alcohol served as models for the diene and dienophile, respectively, and produced Diels–Alder products *in vitro*. Two types of Diels–Alder products were found: (i) when the 1,2-diketone of the quinone acts as the diene in a hetero-Diels–Alder reaction, a benzodioxane structure was produced with a different regiochemistry than the benzodioxane isomer produced *via* radical coupling; (ii) when the quinone's diene participated in the Diels–Alder reaction, a distinctive oxatricyclo structure was produced. Both features may be used as markers for the occurrence of Diels–Alder reactions in lignification. Examination of natural lignins derived from catechyl monomers, however, did not reveal evidence for such products. The conclusion is that the only significant reactions in lignification are combinatorial radical coupling reactions of the single-electron-oxidized phenolics and that polymer chain extension therefore occurs only from the phenolic end-units even in the special case of plants that utilize catechyl monomers for lignification.

Received 20th August 2021,  
Accepted 5th October 2021

DOI: 10.1039/d1gc03022a

rsc.li/greenchem

<sup>a</sup>Department of Energy, Great Lakes Bioenergy Research Center, Wisconsin Energy Institute, Madison, Wisconsin 53726, USA. E-mail: jralph@wisc.edu;

Tel: (+1) 608-890-2429

<sup>b</sup>State Key Laboratory of Pulp and Paper Engineering, South China University of Technology, 381 Wushan Rd, Tianhe District, Guangzhou, 510640, P.R. China

<sup>c</sup>Research Institute for Sustainable Humanosphere, Kyoto University, Gokasho, Uji, 611-0011, Japan

<sup>d</sup>Department of Plant Biotechnology and Bioinformatics, Ghent University, B-9052 Gent, Belgium

<sup>e</sup>Center for Plant Systems Biology, VIB, B-9052 Gent, Belgium

<sup>f</sup>USDA-Forest Service, Southern Research Station, 521 Deval Drive, Auburn, AL 36849, USA

<sup>g</sup>Department of Biochemistry, University of Wisconsin-Madison, Madison, Wisconsin 53706, USA

<sup>h</sup>Department of Biological System Engineering, University of Wisconsin-Madison, Madison, Wisconsin 53726, USA

† Electronic supplementary information (ESI) available: Fig. S1 provides data relating to all possible Diels–Alder products, and Fig. S2–S8 show assigned 1D and 2D NMR spectra establishing the veracity of crucial compound **12**, **12'**, **13**, and **15** assignments. See DOI: 10.1039/d1gc03022a

‡ Current address: Institute of Wood Technology, Akita Prefectural University, 11-1 Aza Kaieizaka, Noshiro, Akita, Japan, 016-0876.

## Introduction

Lignification is the process by which phenolic monomers polymerize, *in planta*, to form lignin polymers.<sup>1–4</sup> The primary canonical monomers, termed monolignols, are *p*-coumaryl, coniferyl, and sinapyl alcohols, hydroxycinnamyl alcohols bearing 0, 1, or 2 methoxyls *ortho* to the phenol (and, consequently, *meta* to the 3-carbon sidechain). After polymerization, these result in the *p*-hydroxyphenyl (H), guaiacyl (G), and syringyl (S) aromatic units in the lignin polymer. The polymerization requires the formation of monolignol, oligolignol, and/or polymer radicals, created by 1-electron oxidation (dehydrogenation) using H<sub>2</sub>O<sub>2</sub>-requiring peroxidases or O<sub>2</sub>-requiring laccases, as shown in Fig. 1A for guaiacyl lignins from coniferyl alcohol **1**. The enzymes do not necessarily need direct contact with the oligomeric/polymeric phenolic substrate, as demonstrated in a manganese peroxidase system in which phenolic radicals were generated *via* a redox shuttle such as Mn(II)/Mn(III) oxalate.<sup>5</sup> Phenolic intermediaries that are more easily oxi-



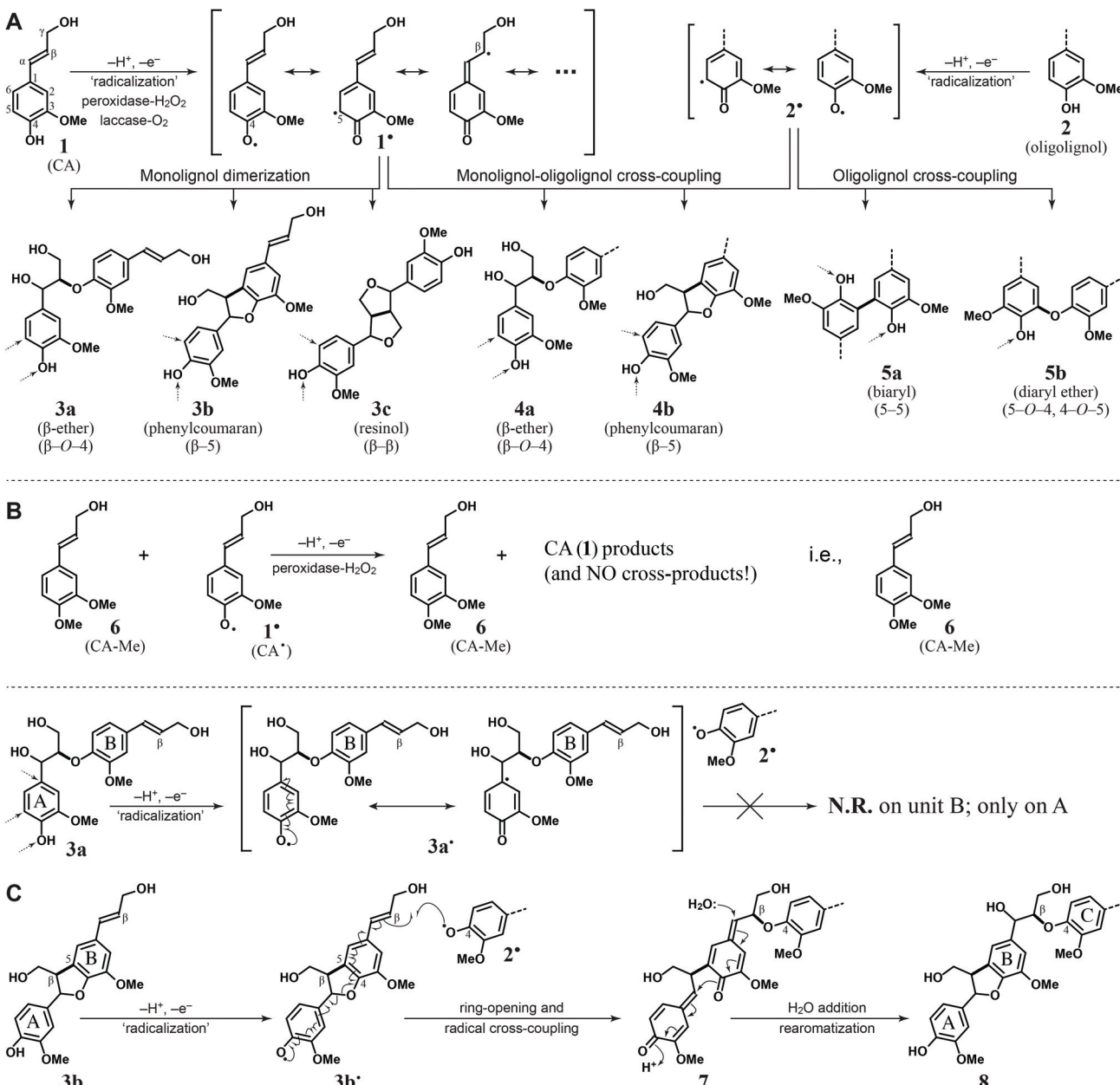


**Fig. 1** (A) Generation of the radical  $1^{\bullet}$  from coniferyl alcohol **1**, a monolignol, and the radical  $2^{\bullet}$  from an oligolignol or lignin chain **2**. Dimerization of **1** (via its radical  $1^{\bullet}$ ) produces, following rearomatization reactions, one of 3 primary dimers **3a–c**; cross-coupling of a monolignol **1** with an oligomer **2** (endwise coupling), the main reaction in lignification, (again via the radicals  $1^{\bullet}$  and  $2^{\bullet}$  of each) lengthens the chain by one unit and produces new end-units **4a–b**; cross-coupling can also join two growing chains **2** to produce 5-5- and 4-O-5-coupled units **5a–b**. The bonds formed during the radical coupling step are highlighted by being bolded. Additional coupling to continue the lignification can occur at the positions noted by the small arrows; obviously, these new products also have the general structure represented by **2**. (B) An attempt to cross-couple a monolignol **1** (via its radical  $1^{\bullet}$ ) with an etherified (phenol-protected) monolignol such as 4-O-methylconiferyl alcohol (3,4-dimethoxycinnamyl alcohol) **6** results in quantitative recovery of starting material **6** along with the usual array of products from the monolignol **1**, i.e., **3a**, **3b**, **3c** as shown in Fig. 2. N.R.: no reaction. (C) What happens to cinnamyl alcohol endgroups in lignification? Top: The usual case is illustrated using a  $\beta$ -ether dimer **3a**. The phenolic radical  $3a^{\bullet}$  can be generated and, as usual, we can understand the coupling pathways available by drawing resonance forms. The resonance form shown illustrates how the single-electron radical density can reach as far as C1, but there is no mechanism by which it can extend into the sidechain. The available coupling possibilities are therefore at 4-O, 5, or 1 (as indicated by the dotted arrows on **3a**). Bottom: A special case in which lignification can occur on an etherified unit.<sup>19</sup> In the phenylcoumaran dimer **3b**, the generated radical  $3b^{\bullet}$  can, via an actual reaction, ring-open and undergo radical coupling at its  $\beta$ -position with a phenolic unit radical  $2^{\bullet}$  to produce, e.g., the intermediate **7**. Following normal rearomatization, the product **8** that appears as though it derives from coupling with the etherified B-unit in **3b**, but it is actually not derived that way (see text).

dized such as *p*-coumarate, or monomer radicals themselves, may also oxidize the polymer by radical transfer.<sup>3,4,6-12</sup>

The subsequent coupling mechanism has some striking features that often surprise organic chemists. First, the polymerization is not a series of radical addition reactions in a chain reaction typified by the polymerization of styrene to polystyrene. Instead, every chain-extension event is a radical coupling (quenching) reaction between two radicals to generate a non-radical neutral species (Fig. 1A); forming a new phenolic radical is required again for the next chain-extension. The apparently energetically profligate process of lignification requires that the newly produced phenolic end-group is again re-oxidized to form a new phenolic radical for further polymerization. A likely advantage of such an apparently energy-inefficient process is that it is controllable, and not subject to runaway radical reactions that are the bane of living systems.

The initial reaction, as illustrated in Fig. 1A for coniferyl alcohol, may be either the (dehydro)dimerization of two monolignol radicals (*via*  $\beta$ - $\beta$ -,  $\beta$ -5-, or  $\beta$ -O-4-coupling) to produce dehydrodimers **3**, or by the cross-coupling of a monolignol radical with any of a variety of initiating or nucleating phenolic monomer radicals (not shown); examples include ferulate (on arabinoxylans, in monocots),<sup>8</sup> and tricin (a flavone, mainly in monocots).<sup>13,14</sup> Here, and in subsequent polymerization, a second striking feature of the lignification mechanism is encountered. The process is a non-enzymatic combinatorial chemical one in the sense that the monomer may couple with another monomer or the growing polymer to form several different products, even if polymerization is from a single monomer type (such as coniferyl alcohol, Fig. 1A); more possibilities arise if the supplied monomer can vary. Ramifications of this combinatorial, chemically-controlled process are noted below.

The major polymerization reaction involves coupling of a monolignol radical with a radical from the phenolic end of a growing polymer **2** (*via* 4-O- $\beta$ - or 5- $\beta$ -coupling) to produce the single-unit-extended polymer **4**. From coupling reactions involving a monolignol, which invariably couples at its  $\beta$ -position, the resulting intermediate products are reactive quinone methides that undergo rearomatization *via* nucleophilic addition at the  $\alpha$ -position by, *e.g.*, water or an internal aliphatic or phenolic hydroxyl group, as typically observed after  $\beta$ -O-4,  $\beta$ - $\beta$ , or  $\beta$ -5 coupling reactions, respectively, to dimers **3a-c** or oligomers **4a-b**. Two lignin chains **2** may also couple at their phenolic ends, *via* 5-5- or 4-O-5-coupling, linking the two chains together and producing units **5** in the polymer (Fig. 1A; the minor  $\beta$ -1 coupling pathway is not shown). By convention, the new bond formed during the coupling reaction ( $\beta$ -O-4,  $\beta$ -5,  $\beta$ - $\beta$ ,  $\beta$ -1, 5-5, and 4-O-5) is used to designate that coupling pathway and the structure in the lignin dimer, or the dimeric unit in an oligomer/polymer, that results following the intermediate's rearomatization.

Under physiological conditions, the radical coupling reactions are considered to be irreversible, as are the following rearomatization reactions, such that the distribution of isomers or of different products reflects kinetic control and

not thermodynamics.<sup>3</sup> For example, if allowed to equilibrate under acidic conditions, both  $\beta$ -guaiacyl and  $\beta$ -syringyl ethers equilibrate to  $\sim$ 50:50 *erythro:threo* (*anti:syn, RS/SR:RR/SS*) thermodynamic ratios, but  $\beta$ -syringyl ethers are produced in approximately 75:25 ratio *in vivo* and under biomimetic *in vitro* conditions, and remain that way in the lignin polymer, as dictated by the kinetics of rearomatization.<sup>3,15</sup>

A key feature of these polymerization reactions is that they are purely chemical and not enzyme- or protein-directed.<sup>1,16,17</sup> The resulting polymer gains two new optical centers each time a monomer couples with another phenolic; as a result of the combinatorial coupling, even from a single type of monolignol monomer, individual polymer chains are structurally and/or stereochemically highly diverse. The complexity is such that even a simple  $\beta$ -ether 20-mer derived from solely  $\beta$ -O-4-coupling reactions to produce a homopolymer has 38 optical centers and consequently  $2^{38}$  optical isomers, or half that many,  $2^{37}$  (over 137 billion), possible physically distinct isomers. Clearly lignin is a very different polymer than, for example, a protein in which every molecule has the same sequence and structure, and is only a single isomer;<sup>18</sup> this is not to say that proteins may not end up becoming different when post-translationally modified, for example. Another corollary of this combinatorial and purely chemical process is that there is no prescribed order of assembly of monomers into the polymer, nor is there any prescribed sequence of the types of units produced by the various coupling regiochemistries available. Because certain couplings are chemically favored over others, the coupling is not, however, statistically random (as sometimes suggested) but reflects coupling and cross-coupling propensities in a statistically weighted manner. As complex as the resulting lignin structure is, however, the lignification process itself is delightfully simple, as only a single chemical mechanism, that of radical coupling, is involved. In many ways lignin biosynthesis is therefore simpler than, for example, the biosynthesis of hemicellulosic polysaccharides.

Even after this mechanism of lignification is accepted, it is still frequently not appreciated that the reaction is exclusively *via* the coupling (quenching) of two radicals (Fig. 1A). Why is it not possible to take a single radical and couple it with a neutral molecule possessing a double bond as in, for example, polystyrene polymerization? Is it possible, for example, to take an etherified monolignol, *i.e.*, one that is phenol-protected, and react it with a monolignol radical (Fig. 1B)? Such reactions are of course known in chemistry, but they involve oxidizing reagents that are considerably stronger than those available in the plant world with its peroxidases and laccases for the process. Lignin chemists have long known that this type of radical cross-reaction (Fig. 1B) will not occur during lignification, but we offer further evidence herein.

A valid question remains, however. Are there viable ways to extend the polymer from an etherified hydroxycinnamyl alcohol at the non-phenolic end of the chain? Traditionally within the lignin literature, the answer is a very strong 'No!' – the double bond of a hydroxycinnamyl alcohol in which its



phenol is etherified is not reactive in a lignification sense. The simple reasoning is that it is not possible for a phenolic radical, generated in a structure containing an etherified hydroxycinnamyl alcohol unit, to propagate any single-electron density to that sidechain double-bond. For example, Fig. 1C, in dimer **3a**, the ring B cinnamyl alcohol is etherified, and therefore cannot enter into any coupling reactions even after generating the ring A phenolic radical **3a'**. In chemical terms, it is not possible to use the mechanistic rules of 'electron-pushing' to transfer single-electron density to the  $\beta$ -carbon in that B-ring double-bond. Recently, however, an apparent exception to this rule in the rather special case of phenylcoumaran dimer **3b** was revealed, Fig. 1C.<sup>19</sup> Because of an actual chemical reaction pathway (not simply resonance), the phenylcoumaran radical **3b'** can ring-open and, in a concerted reaction, undergo radical coupling *via* its B-ring moiety with a phenolic radical **2'**. The result for the example of B $\beta$ -O-4 coupling to give the *bis*-(quinone methide) intermediate **7**, following the usual water addition and re-cyclization of the phenylcoumaran in the rearomatization step, is the apparent extension of the chain *via* the double-bond of a phenol-etherified unit in products such as **8** (Fig. 1C). Preliminary density functional theory (DFT) calculations [at the B3LYP/6-31+G(d) level] indicate that the reaction from **3b'** to **7** is exothermic (at  $-8.65$  kcal mol $^{-1}$ ) indicating that the reaction should occur; the rearomatization reaction to **8** is also obviously energetically downhill. This mechanism had escaped even conjecture until the appearance of the paper revealing this possibility.<sup>19</sup> The evidence from experiments using strategically labeled compounds provides an apparent exception to the rule that phenol-etherified units cannot participate in lignification. It must be stressed, however, that this process involves a true chemical reaction as shown in Fig. 1C. As such, it clearly represents a mechanism by which a phenol-etherified cinnamyl alcohol unit can be involved in a radical coupling reaction and, in addition to occurring in a biomimetic *in vitro* system, almost certainly also occurs during lignification. This eye-opening exception aside, it can still be asserted that, in general, phenol-etherified units cannot inherently generate radicals that can undergo radical coupling, and certainly not by resonance from a distant phenolic radical, *i.e.*, in general, etherified phenolic units cannot participate in the radical coupling reactions of lignification.

Are there other ways in which polymer chain extension might occur on etherified hydroxycinnamyl alcohol end-units in lignins? Interesting candidates may be found in plants deficient in *O*-methyltransferases. Truncated monolignol biosynthesis in such plants produces catechol-containing alternative monomers caffeyl alcohol and 5-hydroxyconiferyl alcohol, resulting in catechyl and 5-hydroxyguaiacyl units (C- and 5H-lignin units) in the polymer. Considerations of the reactivity and polymerization mechanisms of catechyl monomers relate not solely to genetically engineered plants deficient in *O*-methyltransferases, as natural mutants with the same characteristics are well-known in agriculture. The brown-midrib mutants of maize (*bm3* or *bmr3*) and sorghum (*bm12* or *bmr12*) are the classic examples that demonstrate the

plants' utilization of 5-hydroxyconiferyl alcohol monomers in lignification.<sup>20-22</sup> More recently, C-lignin and 5H-lignin polymers derived partially or entirely from caffeyl alcohol or 5-hydroxyconiferyl alcohol have been discovered in the seed-coats of various plants.<sup>23-27</sup> Additionally, the stilbene piceanol, a catechol, has recently been discovered as a lignin monomer in various fruit endocarp tissues and bark.<sup>28-31</sup> We reasoned that such catechyl monomers could produce *ortho*-benzoquinones under the dehydrogenative (oxidative) conditions of lignification; quinones, including *o*-quinones, are known plant metabolites.<sup>32</sup> Indeed, early on it was contended that such catechyl monomers, if produced, would spontaneously oxidize or disproportionate to *o*-benzoquinones that could not then undergo radical coupling reactions and therefore lignification in a normal sense.<sup>33,34</sup> The incorporation of the catechyl monomers into the single-electron oxidative processes of lignification has, however, been decisively confirmed, as reviewed.<sup>3,4,12,35</sup> Nevertheless, we hypothesized that *o*-benzoquinones, if formed, could readily act as the diene component of classical Diels–Alder reactions, with cinnamyl alcohol units, even those present in etherified structures, being the required dienophile, analogously to reported reactions of galloyl quinones.<sup>36</sup> Aqueous intermolecular Diels–Alder reactions are known.<sup>37</sup> We report here a demonstration that, in the special case of catechyl monomers reacting with etherified hydroxycinnamyl alcohols, *in vitro* Diels–Alder reactions can indeed occur and produce diagnostic marker units for such reactions. We then explore whether such reactions can be found to occur during *in planta* lignification.

## Results and discussion

The major goal of this research was to establish whether there were plausible mechanisms by which, under special circumstances, etherified hydroxycinnamyl alcohol units in lignins might participate in lignification. We were particularly interested in determining whether lignification with catechyl monomers could, *via* their *o*-benzoquinones, open up the possibility of Diels–Alder reactions in addition to the prototypical radical coupling reactions. We first needed to reaffirm that etherified hydroxycinnamyl alcohols cannot and do not participate in radical coupling reactions under lignification conditions.

### Establishing that etherified monolignols do not normally participate in lignification

Here we attempt to show a feature that is well-known in the lignin field, namely that cinnamyl alcohols without the (conjugated) phenolic-OH group cannot form radicals under lignification conditions and nor can they somehow cross-couple with a (phenolic) radical, *i.e.*, that etherified hydroxycinnamyl alcohol moieties cannot participate in lignification. We took coniferyl alcohol **1** and 4-*O*-methylconiferyl alcohol **6** (=3,4-dimethoxycinnamyl alcohol) in a biomimetic peroxidase/H<sub>2</sub>O<sub>2</sub> *in vitro* system (Fig. 1B) wherein, as shown in Fig. 2, the coni-



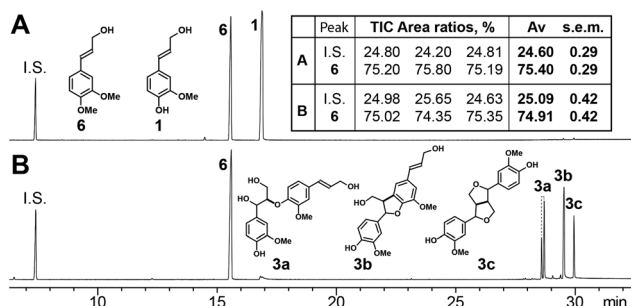


**Fig. 2** Total-ion chromatogram of (A) starting mixture and (B) product mixture, showing that 4-O-methylconiferyl alcohol **6** does not participate in radical coupling reactions whereas coniferyl alcohol **1** is converted by the biomimetic peroxidase-H<sub>2</sub>O<sub>2</sub> system to dimers by coupling  $\beta$ -O-4 (**3a**, two isomers, *syn* or *threo*, *anti* or *erythro*),  $\beta$ -5 (**3b**, one isomer, *trans*), and  $\beta$ - $\beta$  (**3c**, one isomer). I.S.: 3,4-dimethoxybenzaldehyde. Average, s.e.m. (standard error of the mean) from 3 replicates.

Coniferyl alcohol **1** undergoes dehydromimerization to produce four dimers **3**, the two isomers of the  $\beta$ -ether **3a**, and the single isomers each of the phenylcoumaran **3b** and the resinol **3c**. Coniferyl alcohol's phenol-methylated analog, 4-O-methylconiferyl alcohol **6**, remains totally intact; quantification of **6** before and after reaction (in triplicate) reveals that it has not reacted, and no cross-products from it were observed. We hope that this demonstration will be sufficiently convincing to confirm the contention that a free phenol is required for radical coupling, and perhaps avert further notions of cross-coupling reactions with etherified components from being entertained in the lignin literature.

### Possibility of Diels–Alder reactions between the double-bond of a cinnamyl alcohol as the dienophile and an *o*-benzoquinone as the diene

Catechyl structures can potentially be oxidized to form *o*-benzoquinones under the dehydrogenative (oxidative) conditions of lignification (Fig. 3). Horseradish peroxidase oxidized catechol to *o*-benzoquinone *in vitro*, for example.<sup>38</sup> A Diels–Alder reaction is a concerted [4 + 2] addition reaction between a conjugated diene and an alkene, the latter of which is termed a dienophile. Ideally, one of the pair is electron-deficient (substituted with electron-withdrawing groups) and the other is electron-rich (substituted with electron-donating groups). In the case of *o*-benzoquinones derived from catechyl monomers in lignification, obviously the quinone is electron-deficient, whereas the monolignol is electron-rich. An *o*-benzoquinone has two modes by which it may act as a diene – the actual diene itself in the traditional Diels–Alder reaction, or the 1,2-diketone in a so-called hetero-Diels–Alder reaction.<sup>39,40</sup> Such cycloaddition reactions have even been noted in a somewhat lignin-related sense.<sup>41</sup> After initially discovering a Diels–Alder product in an attempted *in vitro* radical coupling reaction between coniferyl alcohol **1** and methyl 5-hydroxyvanillate **11**, as will be described below, we undertook a more careful evaluation of the products from a simple etherified analog of coniferyl alcohol, 4-

O-methylconiferyl alcohol **6** (Fig. 3), and the *o*-benzoquinone **9** derived explicitly from methyl 5-hydroxyvanillate **11** under oxidative conditions and isolated before the reaction.

### Initial discovery of a Diels–Alder product from an attempted *in vitro* radical cross-coupling reaction between coniferyl alcohol and methyl 5-hydroxyvanillate

Early in the process of characterizing lignins in COMT-deficient plants we attempted to make compounds to authenticate the new benzodioxane units being discovered.<sup>22–24,26,29,42–49</sup> We sought the benzodioxane product **12'a** (Fig. 3) as an intermediate compound to synthesize such a benzodioxane lignin model compound.<sup>42</sup> By cross-coupling coniferyl alcohol **1** with methyl 5-hydroxyvanillate **11**, we also isolated (unreported at the time) a modest (5%) yield of a product that had as many as nine HMBC NMR correlations to some of its protons – see later in Fig. 5 and 7. We deduced this product to be the trimer **15** (Fig. 3), as reported here (below) for the first time, a Diels–Alder [4+2]-cycloaddition product. Two possible reaction pathways, which cannot be distinguished here, could lead to this product. Coniferyl alcohol **1** could directly undergo a Diels–Alder reaction with quinone **9** (formed by *in situ* oxidation of catechol **11** under the dehydrogenation conditions) to form compound **13a** which could then subsequently chain-elongate to **15** *via* radical coupling as usual between the phenolic radical of **13a** and a further radical from coniferyl alcohol **1**. Alternatively, two coniferyl alcohol **1** monomers could first dimerize *via* radical coupling to the  $\beta$ -5 (phenylcoumaran) dehydromimer **14**, which could then subsequently act as a dienophile in a Diels–Alder reaction with diene **9** to produce **15**. Compound **13a** was not isolated from the mixture but that doesn't discount its possible intermediacy. We assume, but did not verify, that higher oligomers of coniferyl alcohol that, like compound **14**, retain the cinnamyl alcohol end-unit, could also undergo the Diels–Alder reaction with diene **9** to form higher-molecular-mass products. We discuss the nature of the trimer **15** and the production of benzodioxanes from either radical coupling or Diels–Alder cyclization below after first examining the simpler reaction depicted in the top line of Fig. 3.

### Diels–Alder products from the coupling of 4-O-methylconiferyl alcohol and the quinone from methyl 5-hydroxyvanillate

After the observation that the Diels–Alder product **15** was produced in our attempts to cross-couple coniferyl alcohol **1** and methyl 5-hydroxyvanillate **11**, we more carefully examined the pathway and products from the reactions between a simpler phenol-protected monolignol, 4-O-methylconiferyl alcohol **6** (that could not be involved in radical coupling reactions because it lacks the requisite phenol), and the quinone **9** (Fig. 3). The quinone **9** was therefore generated explicitly from methyl 5-hydroxyvanillate **11** and isolated before the reaction.

Reaction of quinone **9** with **6** at room temperature produced a mixture of four main products (Fig. 3, top row) for which structures could readily be determined by NMR analysis. In addition to the starting material **6**, one product was 4-O-

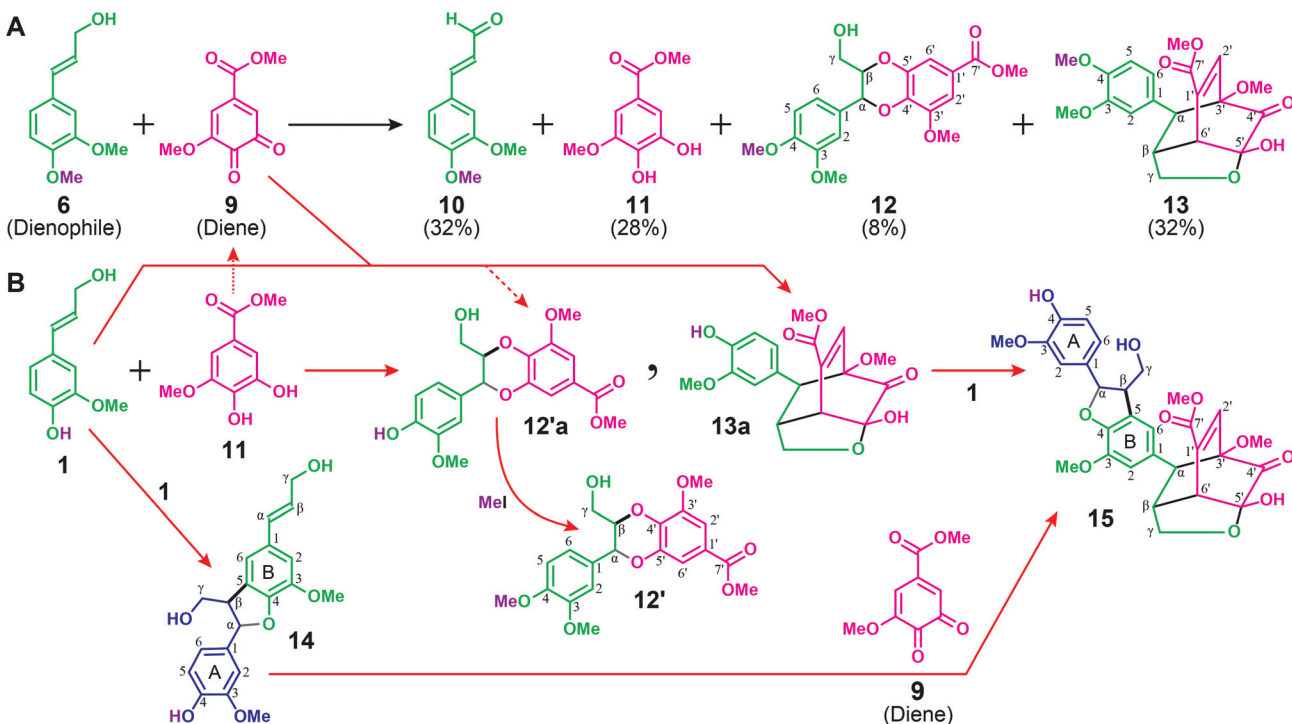


**Fig. 3** Diels–Alder reaction between a quinone and a cinnamyl alcohol. (A) In the top line (black reaction arrows) are the reaction products from reacting 4-*O*-methylconiferyl alcohol **6** with the quinone **9** from catechol **11** (methyl 5-hydroxyvanillate). Notably, two Diels–Alder products are formed: a benzodioxane **12** and an oxatricyclo compound **13**. Percentages are relative to the total yield of the four products (which totals 100%); actual yields are provided in the Experimental section. (B) The bottom scheme (red reaction arrows) is from the attempted reaction of coniferyl alcohol **1** with catechol **11** to produce the  $\beta$ -*O*-4-coupling product, benzodioxane model **12'a**, from which was isolated Diels–Alder product **15**; compound **15** could be produced via first producing either **14**, the  $\beta$ -5 dimer of coniferyl alcohol, followed by Diels–Alder coupling with quinone **9**, or via Diels–Alder product **13a** followed by radical coupling with further coniferyl alcohol **1**. Methylation of benzodioxane **12'a** produced the benzodioxane **12'**, which is an isomer of **12**. In other words, the Diels–Alder reaction product, benzodioxane **12**, that resembles a radical coupling product is not the same product **12'** that is produced by radical coupling (followed by simple phenol-methylation). Compounds are colored green to show the units sourced from the cinnamyl alcohol **1** (but dark blue for the second coniferyl alcohol **1** moiety added) and magenta from the quinone **9** or catechol **11**; black bonds are those created in the [4+2]-cycloaddition reaction or from the subsequent internal trapping of the diketone by the  $\gamma$ -OH; the bold black bond in **12'a**, **12'**, **14** and **15** is the bond formed during radical coupling of coniferyl alcohol **1**, and the gray bonds are from the internal cyclization (rearomatization) of the quinone methide intermediate.

methylconiferaldehyde (3,4-dimethoxycinnamaldehyde) **10**, with its diagnostic aldehyde peak at 9.65 ppm in the  $^1\text{H}$  NMR spectrum. This compound derived from the oxidation of compound **6** by the quinone **9**, as corroborated by also finding the reduction product, catechol **11**. The third product was the 1,4-benzodioxane **12**. In the  $^1\text{H}$  NMR spectrum, the  $\alpha$  and  $\beta$  proton peaks were observed at 5.01 and 4.07 ppm (Fig. 8), similarly to those found in some 1,4-benzodioxane structures in lignin and neolignans, and analogously to benzodioxanes prevalent in the recently discovered C-lignin and 5H-lignin in certain seedcoats.<sup>23–27</sup> This compound **12** was determined to be a *trans*-stereoisomer by the coupling constant between protons  $\alpha$  and  $\beta$  ( $J = 8.17$  Hz); the *cis*-isomer of **12** cannot be formed *via* a concerted Diels–Alder reaction with *trans*-4-*O*-methylconiferyl alcohol **6** as the dienophile. Without the presence of a phenolic-OH on compound **6**, it was concluded that this benzodioxane structure **12** had to have been formed by the Diels–Alder reaction between the diketone of the *o*-benzoquinone **9** and the alkene in **6**, *i.e.*, that quinone **9** is capable of reacting as a

diene in two senses; in this case it is the 1,2-diketo system that is the diene in a ‘hetero-Diels–Alder’ reaction.<sup>39,40</sup> However, benzodioxane **12** was a regioisomer of the analogous product formed by radical coupling – see below.

The final product was the expected oxatricyclo Diels–Alder product **13** (Fig. 3, 6, and S2†). In this case, it is the conjugated diene itself that has acted as the diene in the Diels–Alder reaction, quite analogously to reported reactions of galloyl quinones.<sup>36</sup> The structure was determined by NMR analysis using normal assignment principles from the typical array of 1D and 2D NMR experiments –  $^1\text{H}$  (Fig. S2†),  $^{13}\text{C}$  (Fig. S4A†), COSY (Fig. 4A), NOESY (Fig. 4B), HSQC (Fig. 5, red contours), and HMBC (Fig. 5, black contours). Confirmation was from reported  $^1\text{H}$  NMR data of a compound that has the common oxatricyclo structure.<sup>50</sup> In the COSY spectrum (Fig. 4A), proton  $2'$  correlated with protons  $\alpha$  and  $6'$ , but not with the  $\beta$  proton. Proton  $\beta$  correlated with protons  $\alpha$ ,  $6'$ , and  $\gamma$ , but not with the  $2'$  proton. These data strongly suggest that protons  $2'$  and  $\beta$  are the most separated in the proton coupling network. In the



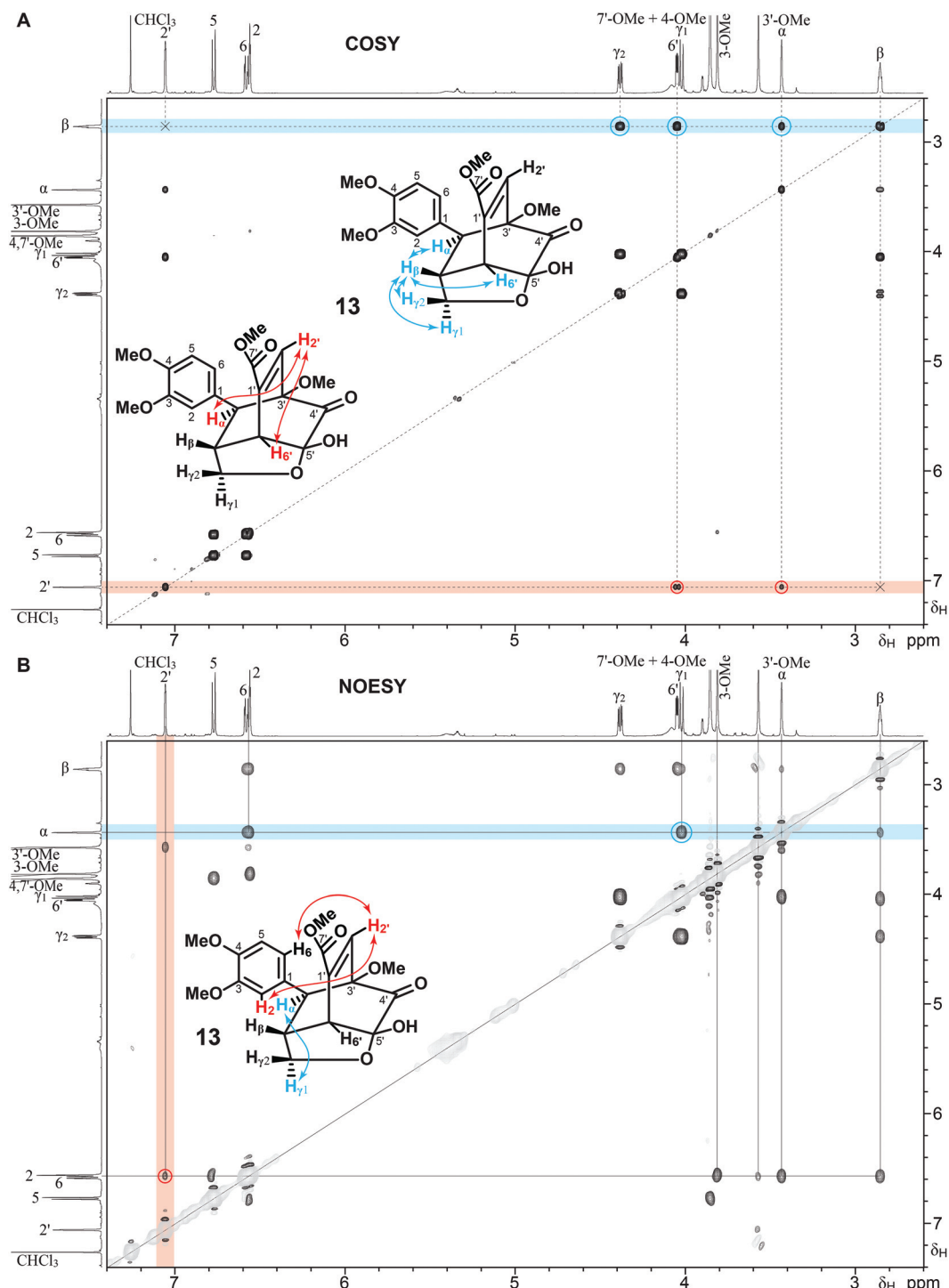


**Fig. 4** COSY and NOESY spectra of compound **13** (500 MHz, in  $\text{CDCl}_3$ ). (A) COSY spectrum highlighting correlations between protons 2' (red) and  $\beta$  (cyan). (B) NOESY spectrum highlighting correlations between protons 2' and 6 and/or 2 (red), and between protons  $\alpha$  and  $\gamma_1$  (cyan); negative contours, mainly associated with the diagonal and devoid of useful information, are in a light gray to deemphasize them.

NOESY spectrum (revealing protons that are spatially close, Fig. 4B), proton 2' correlated with protons 2 and 6 (as well as the 3'-OMe). Proton  $\alpha$  correlated with proton  $\gamma_1$  but not with proton  $\gamma_2$  (Fig. 4B), observations that are also consistent with the structure **13** drawn. Further confirmation was provided by

the carbon 2' correlations in the HMBC spectrum that are generally limited to 3-bonds (Fig. 5); Carbon 2' correlated with protons 6' and  $\alpha$ , but not with proton  $\beta$ . HMBC spectra are particularly diagnostic of these types of Diels–Alder products (such as **13**) because of the incredible number of correlations

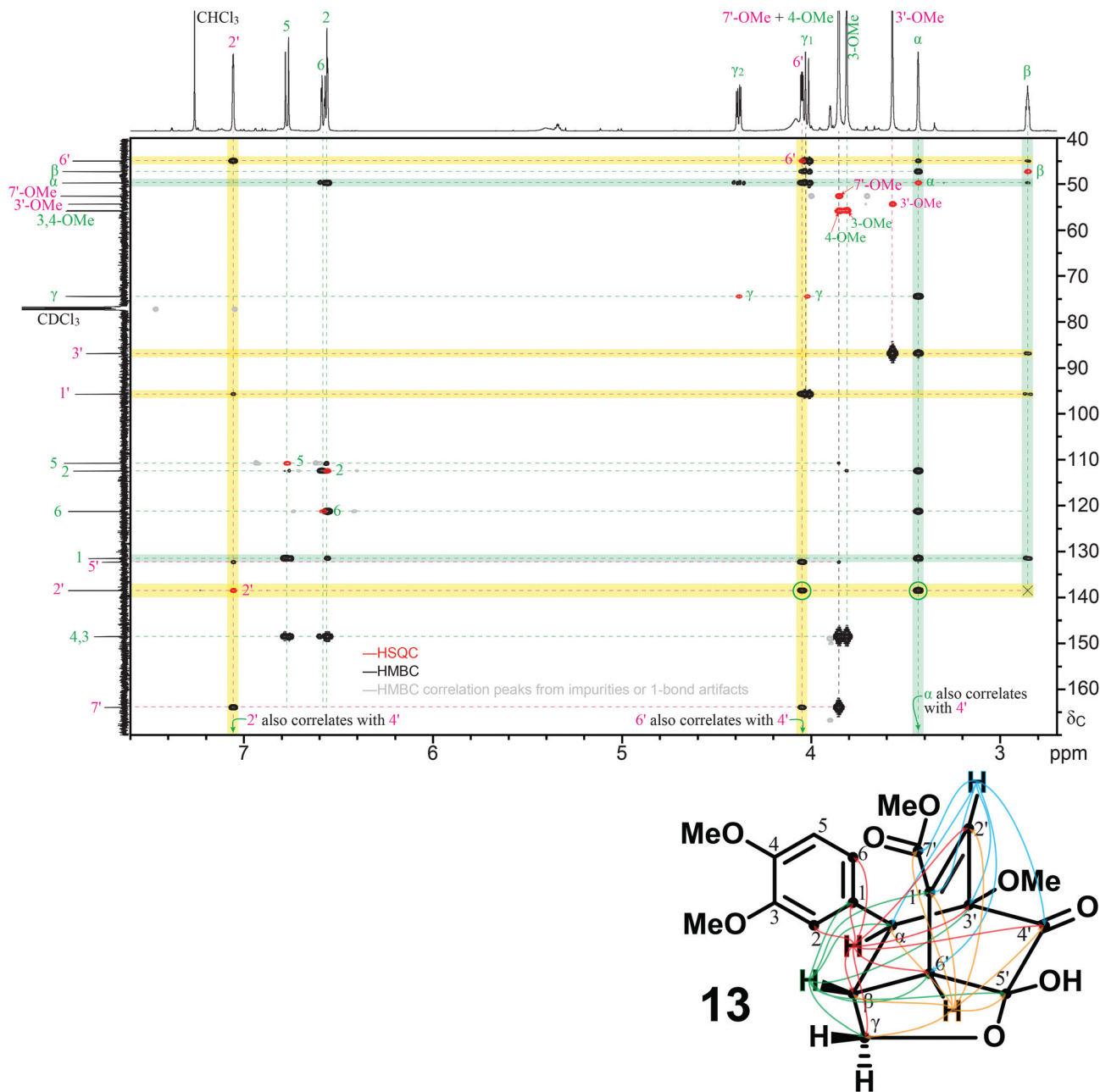


**Fig. 5**  $^1\text{H}$ – $^{13}\text{C}$  correlation spectra of compound **13** (500 MHz, in  $\text{CDCl}_3$ ). HSQC (red contours, and with assignments) and HMBC spectra (black) showing 3-bond correlations of protons  $6'$  (yellow highlighting) and  $\alpha$  (green highlighting) to carbon  $2'$  that are useful for defining the stereochemistry. Bicyclo[2.2.2]octanes (including **13** here) from Diels–Alder reactions have HMBC correlations between a proton and carbons 2- or 3-bonds separated that initially seem to be too numerous to be physically possible, but are in fact beautiful signatures of such structures. For example, as shown by the green and yellow shading, proton  $\alpha$  correlates with *nine* carbons:  $6'$ ,  $\beta$ ,  $\gamma$ ,  $3'$ ,  $2$ ,  $6$ ,  $1$ ,  $2'$ , and  $4'$  (in chemical shift order); the correlation to  $4'$  is too distant to be shown in this plot region (but is present). Similarly, proton  $\beta$  correlates with *five* carbons:  $6'$ ,  $\alpha$ ,  $3'$ ,  $1'$ , and  $1$ ; the  $2'$  proton correlates with *five* carbons:  $6'$ ,  $1'$ ,  $5'$ ,  $7'$ , and  $4'$ ; and proton  $6'$  correlates with *seven* carbons:  $\beta$ ,  $\alpha$ ,  $1'$ ,  $5'$ ,  $2'$ ,  $7'$ , and  $4'$ . Contours colored light gray are from residual 1-bond correlations (split by the 1-bond  $^1\text{H}$ – $^{13}\text{C}$  coupling constant) from some peaks due to deviation from the set average value (145 Hz); darker gray contours are from minor impurities. The structure below shows the complex color-coded HMBC correlations from protons in the oxatricyclo ring to carbons within 3-bonds, also confirming its regiochemical assignment of compound **13**.

possible between protons and carbons that are within 3-bonds of each other; proton  $\alpha$ , for example, correlates with nine carbons,  $6'$ ,  $\beta$ ,  $\gamma$ ,  $3'$ ,  $2$ ,  $6$ ,  $1$ ,  $2'$ , and  $4'$  – all but the  $4'$  correlation (that was nevertheless observed, as indicated) are shown in Fig. 5.

## Rationalization of Diels–Alder coupling to produce a single isomer of product 13

The Diels–Alder possibilities for reaction of the diene **9** with dienophile **6** are referred to as being ‘inverse electron-demand’

Diels–Alder reactions because the diene is electron-deficient and the dienophile is electron-rich, well known reactions that are opposite to the originally reported ‘conventional’ or ‘normal electron-demand’ reaction.<sup>51,52</sup> In the case of the Diels–Alder reaction in which the conjugated double-bonds (and not the quinone system) in *o*-benzoquinone **9** act as the diene, four products from the cycloaddition with dienophile **6**, two bicyclo isomers and two oxatriacyclo isomers, can be drawn (Fig. S1†). However, the only Diels–Alder product is that anticipated and rationalized if the reaction is considered to be ionic (as most readily visualized *via* the gray arrows and resonance forms drawn in Fig. 6A), *i.e.*, the oxatriacyclo product **13**. The concerted Diels–Alder cycloaddition reaction is shown by the magenta arrows; the alternative orientations (Fig. S1B–D†) simply don’t comport with the electronics. NMR confirms this structure **13** as the main/sole Diels–Alder product of this type obtained, clarifying that the Diels–Alder reaction can occur

using the diene in the quinone structure **9** and the double-bond in the 4-*O*-methylconiferyl alcohol **6** as the dienophile. As noted above, the Diels–Alder reaction in which the diketone in **9** can act as the diene is also produced, as discussed below.

Molecular modeling can also be used to help rationalize the products **12** and **13** observed from the Diels–Alder coupling of 4-*O*-methylconiferyl alcohol **6** and quinone **9**, Fig. 3 and 6. Firstly, the proposed inverse electron-demand nature of this Diels–Alder system in which the LUMO of the diene and the HOMO of the dienophile is confirmed by a much smaller gap between these frontier molecular orbitals. Next, per the experimental results, compound **13** is the main Diels–Alder product, with the benzodioxane **12** also detected. Computationally, **12** is the more stable by 8.1 kcal mol<sup>−1</sup> (Fig. 6). This relatively large thermodynamic difference is probably due to the retention of two aromatic rings in the benzodioxane. Among the bicyclic and tricyclic Diels–Alder adducts the tricyclic com-

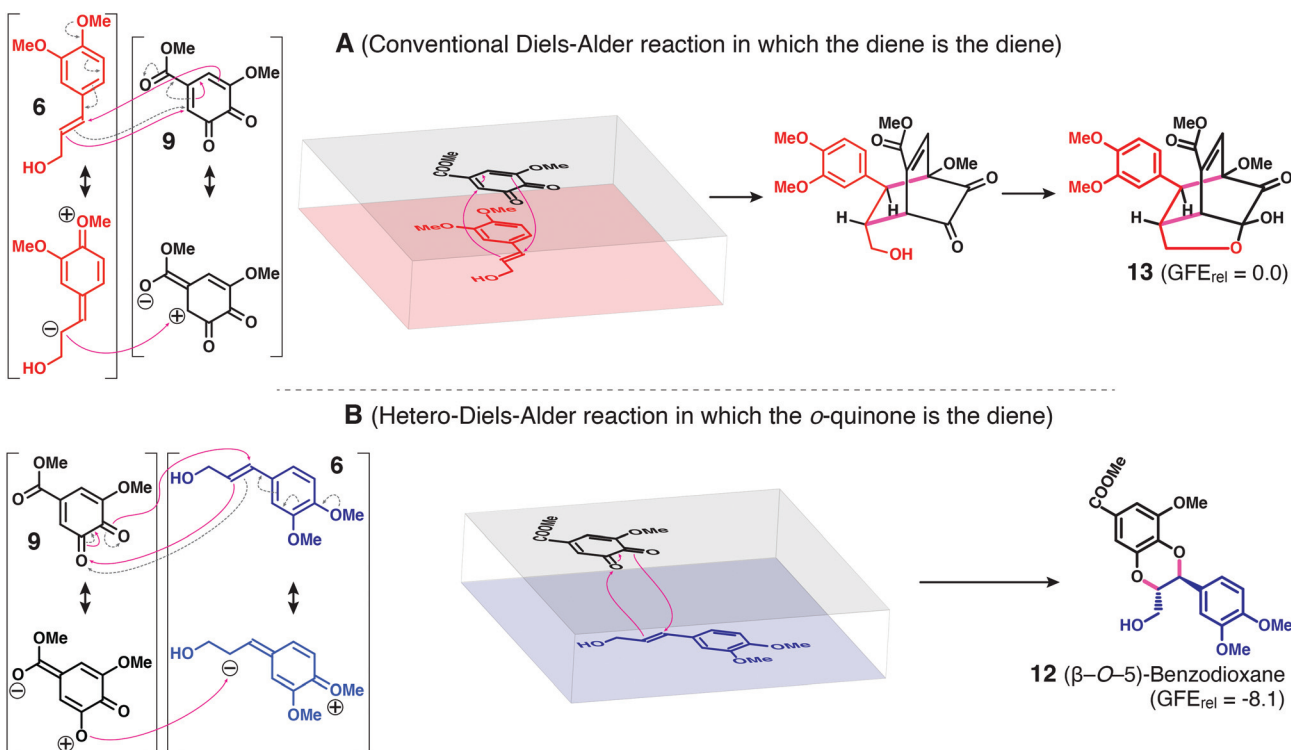


**Fig. 6** Diels–Alder reactions and products from 4-*O*-methylconiferyl alcohol **6** and the quinone **9** from methyl 5-hydroxyvanillate **11**. Two so-called ‘inverse electron-demand’ (because the diene is electron-deficient and the dienophile is electron-rich) Diels–Alder reactions are possible. (A) The conventional Diels–Alder reaction in which the diene itself acts as the diene component. Because of the electronic requirements (see text), there is a strongly favored regiochemical possibility, producing **13** (and its optical isomer). (B) The ‘hetero-Diels–Alder’ reaction in which the *o*-benzoquinone acts as the diene. To satisfy the electronic requirements, the regiochemistry, if it were described as resulting from radical coupling, appears as a β-O-5 product **12**; because of the concerted nature of the reaction, strictly *trans*-benzodioxane **12** is produced. The regiochemistry and the *trans*-only nature of the benzodioxane ring are therefore significantly different from the outcome with radical coupling, in which only the β-O-4 coupling product **12'** (Fig. 3, and see later in Fig. 8) is produced, and in which the ring-closure from the quinone methide intermediate allows both *trans*- and *cis*-benzodioxane rings to form, admittedly with the *cis*-ring being minor (~5%). Modeling doesn’t allow a prediction of a favored benzodioxane as the Gibbs free energy (GFE) levels are similar (Fig. S1†); lower GFEs are predicted for both benzodioxanes **12** and **12'** than for the conventional Diels–Alder product **13**, also proving to be of limited value given that the latter is the major product. Note: In the structures on the left (and also in the orientational figures in the middle), the magenta arrows show the conventional concerted Diels–Alder electron-pushing with the anticipated (and observed) regiochemistry from electronic considerations, whereas the dashed gray arrows indicate (part of) the ionic rendition – a useful tool for predicting the reaction regiochemistry [see, for example, [https://en.wikipedia.org/wiki/Diels–Alder\\_reaction](https://en.wikipedia.org/wiki/Diels–Alder_reaction)]. The full range of potential products is shown in Fig. S1†.



pounds are the most stable, and compound **13** is the most stable among these. Despite the energy calculations suggesting that the benzodioxane **12** is significantly more stable than the oxatricyclo product **13**, both products were observed in comparable amounts (with **13** predominating) implying that both of these Diels–Alder reactions can occur between these two substrates, and with roughly similar propensities.

### Diels–Alder coupling reactions produce trimer **15**

As seen from the NMR data, the product **13** (Fig. 4, 5 and Fig. S2, S4A†) from reaction of 4-*O*-methylconiferyl alcohol **6** and quinone **9** (Fig. 3) and the product **15** (Fig. 7 and Fig. S3, S4B†) isolated from the reaction of coniferyl alcohol **1** with catechol **11** (*via* its quinone **9** and involving at least one coniferyl alcohol radical to produce the  $\beta$ -5 moiety), share significant structural similarities, particularly with the oxatricyclo moiety. In each case, the regiochemistry of the reaction can be defined from particularly the HMBC correlations observed, Fig. 5 and 7, and are supported by NOESY correlations. Particularly striking again are the HMBC correlations between proton  $\alpha$  in **13** and proton  $\text{B}\alpha$  in **15** with all nine carbons within 3 bonds of it in each case (Fig. 5 and 7).

It is perhaps evident in the 1D projections on Fig. 7, but is more clearly revealed in the 1D spectra in Fig. S3 and S4B,† that most of the proton and carbon multiplets in the spectra of **15** are split into two resolved sets each. This is because there are two isomers in essentially equal proportion, but it might not be obvious how these arise. There are clearly two stereocenters (at  $\text{A}\alpha$  and  $\text{A}\beta$ ) in the phenylcoumaran moiety, and five in the oxatricyclo system. However, because these are all constrained relative to each other in each moiety, it is equivalent to having just one stereocenter in the phenylcoumaran and one in the oxatricyclo system, but these are independent of each other, so they could be like *RR/SS* and *RS/SR* isomers (as are *syn* and *anti*, or *threo* and *erythro* isomers, for example). As shown in Fig. 7, it appears that the phenylcoumaran moiety in **15** is in the *trans*-configuration (because there is only one real isomer of the dimer **14**, Fig. 3) such that  $\alpha\beta$  is either *RS* or *SR*. The stereochemistry of the oxatricyclo system of **15** in the order  $3'$ ,  $\text{B}\alpha$ ,  $\text{B}\beta$ ,  $6'$  appears to be *SRRR/RSSS*. The two isomers combined would be the two pairs of optical isomers *RSSRRR/SRRSSS* and *SRSRRR/RSRSSS*. Again, it is easiest to equate this compound to having a single optical center in each moiety, as with typical *threo/erythro* or *syn/anti* isomer pairs. Incidentally, we have previously seen this NMR separation of isomers in which the two optical centers, even when separated by many bonds within the molecule, are in separate moieties, as will be revealed separately (unpublished).<sup>53</sup>

### Benzodioxanes resulting from hetero-Diels–Alder vs. radical coupling

Since their original discovery in lignins,<sup>42–44,54</sup> benzodioxane units are now well-known to result from lignification in which catechyl lignin monomers such as caffeyl alcohol or 5-hydroxyconiferyl alcohol are involved; as noted above, certain seedcoat

lignins are derived solely from such monomers resulting in lignins that are almost exclusively composed of benzodioxane units.<sup>23–27</sup> In lignins and in model reactions, they have always been described to be the benzodioxanes derived from 4-*O*- $\beta$ -coupling of the catechol with a monomer. Although theoretically possible, the 5-*O*- $\beta$ -coupled benzodioxane isomers have not been described to occur. The rationalization is that the product derives from the more conjugated (and therefore more stable) 4-*O*-radical, even though radical transfer to produce the presumably more reactive 5-*O*-radical would be energetically trivial.

The benzodioxane **12** produced by the Diels–Alder reaction between 4-*O*-methylconiferyl alcohol **6** and the *o*-benzoquinone **9** from methyl 5-hydroxyvanillate **11** can be described as a 5-*O*- $\beta$  or  $\beta$ -*O*-5 product (were it to derive from radical coupling, Fig. 3). This structure was particularly evidenced by the 3-bond HMBC correlations between proton  $\alpha$  and carbon  $4'$ , and between proton  $\beta$  and carbon  $5'$  (Fig. 8A, the carbon assignments of which can be quite unambiguously assigned by first principles, *i.e.*, without resorting to chemical shift arguments, by analysis of the combined correlation data from the various experiments). To confirm the structure of the radical coupling product **12'a** (Fig. 3) between coniferyl alcohol **1** and methyl 5-hydroxyvanillate **11**, we methylated its phenolic-OH using methyl iodide, thereby creating the isomer **12'** (Fig. 3). In contrast to its Diels–Alder-produced counterpart **12**, the HMBC correlations in **12'** were between proton  $\alpha$  and carbon  $5'$ , and between proton  $\beta$  and carbon  $4'$  (Fig. 8B), establishing **12'a** firmly as the 4-*O*- $\beta$ -coupling product.

Clearly, the Diels–Alder reaction and the radical coupling pathway produced opposite geometric isomers. Another observation was that radical coupling produced some 5% of the *cis*-benzodioxane ring (Fig. 8B) whereas we noted (and can fully rationalize) only the *trans*-benzodioxane from the Diels–Alder reaction. Although we cannot unambiguously claim that there was no *cis*-isomer of **12**, it is logical that there was none as the stereochemistry of the benzodioxane ring is fully defined by the concerted [4+2]-cycloaddition reaction. The exciting realization is that we now have two product structures (the  $\beta$ -*O*-5-benzodioxane as in **12**, and the oxa-tricyclo unit as in **13**) that, if found in lignin, would be diagnostic for the occurrence of Diels–Alder reactions during lignification, and perhaps the *cis*-(4-*O*- $\beta$ )-benzodioxane is a ‘marker’ for radical coupling. That said, because of the similarity of the spectra and the closely matched correlations in the HSQC spectra, Fig. 8, we don’t expect to be able to resolve and distinguish the two possibilities in the broader HSQC spectra from actual lignins.

### Are Diels–Alder reactions produced in lignification that involves catechyl monomers?

Plants’ utilization of catechyl monomers in lignification has been noted in mutants or transgenics deficient in *O*-methyltransferases,<sup>20,43</sup> as we’ve reported in a number of reviews.<sup>3,4,11,12,17,18,55,56</sup> In two independent studies, *Arabidopsis* was engineered to derive its lignin from 5-hydroxyconiferyl alcohol.<sup>57,58</sup> Whereas the levels of 5-hydroxyguaiacyl

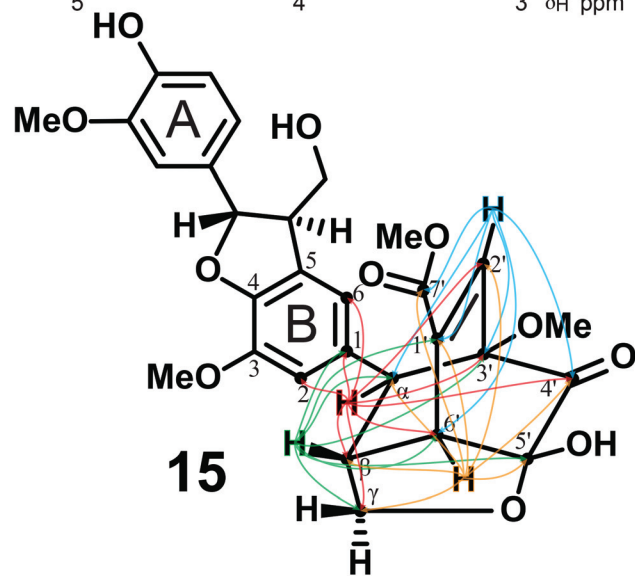
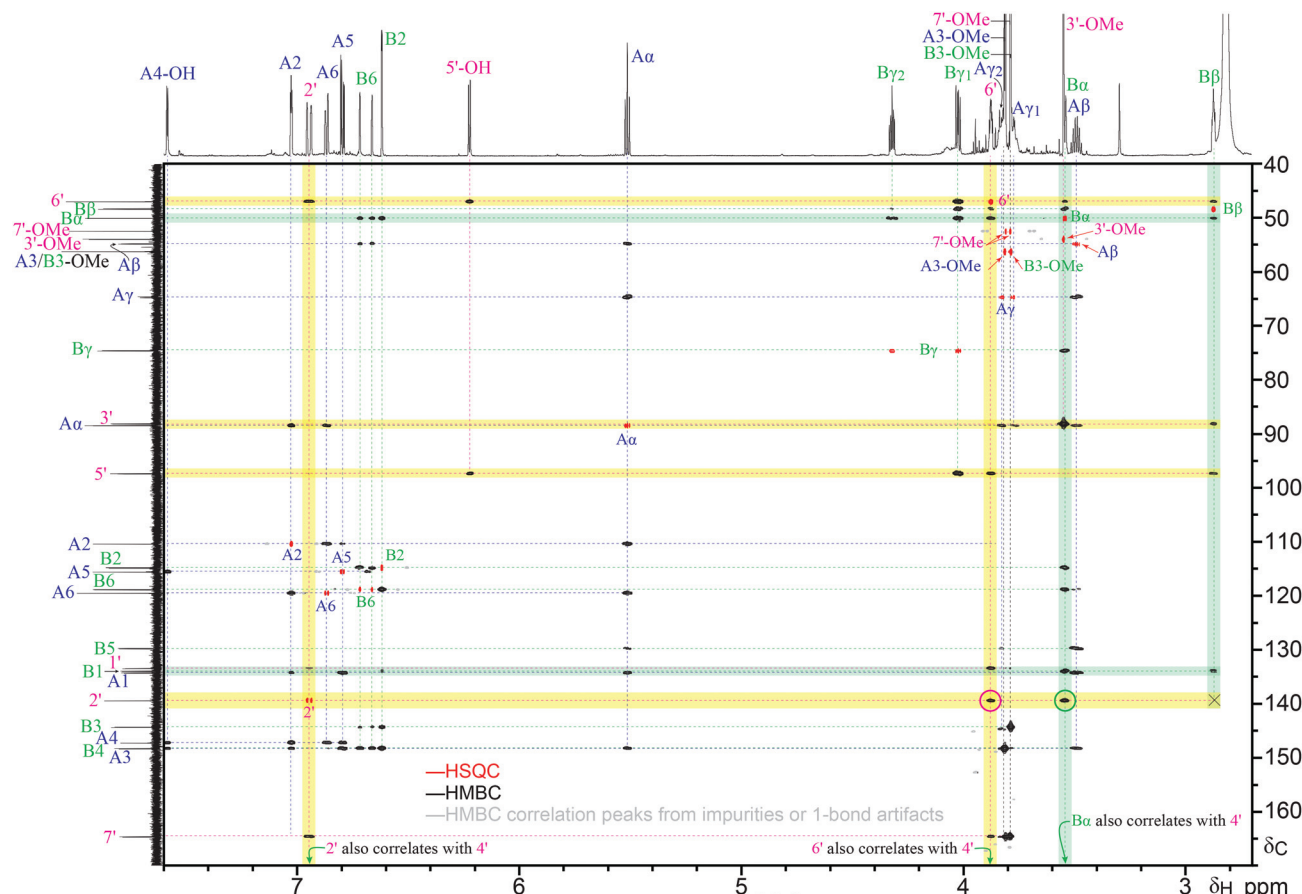


**Fig. 7**  $^1\text{H}$ – $^{13}\text{C}$  correlation spectra of compound 15 (700 MHz, in acetone- $d_6$ ). HSQC (red contours, and with assignments) and HMBC spectra (black) showing (with green highlighting) correlations of protons 6' and  $\text{B}\alpha$  to carbon 2' that are useful for defining the stereochemistry. Bicyclo[2.2.2]octanes (including 15 here) from Diels–Alder reactions have HMBC correlations between a proton and carbons 2- or 3-bonds separated that initially seem to be too numerous to be physically possible, but are in fact a beautiful signature of such structures. For example, as shown by the green shading, proton  $\text{B}\alpha$  correlates with *nine* carbons: 6',  $\text{B}\beta$ ,  $\text{B}\gamma$ , 3', B2, B6, B1, 2', and 4' (in chemical shift order); the correlation to 4' is too distant to be shown in this plot region but is clearly seen in the data. Similarly, proton  $\text{B}\beta$  correlates with *six* carbons: 6',  $\text{B}\alpha$ ,  $\text{B}\gamma$  (weak, and below the level drawn in the figure), 3', 5', and B1; the 2' proton correlates with *five* carbons: 6', 5' (weak, and below the level drawn in the figure), 1', 7', and 4'; and proton 6' correlates with *seven* carbons  $\text{B}\beta$ ,  $\text{B}\alpha$ , 5', 1', 2', 7', and 4'. Contours colored light gray are from residual 1-bond correlations (split by the 1-bond  $^1\text{H}$ – $^{13}\text{C}$  coupling constant) from some peaks due to deviation from the set average value (145 Hz); darker gray contours are from minor impurities. The structure below shows the complex color-coded HMBC correlations from protons in the oxatricyclo ring to carbons within 3-bonds, also confirming its regiochemical assignment of compound 15.



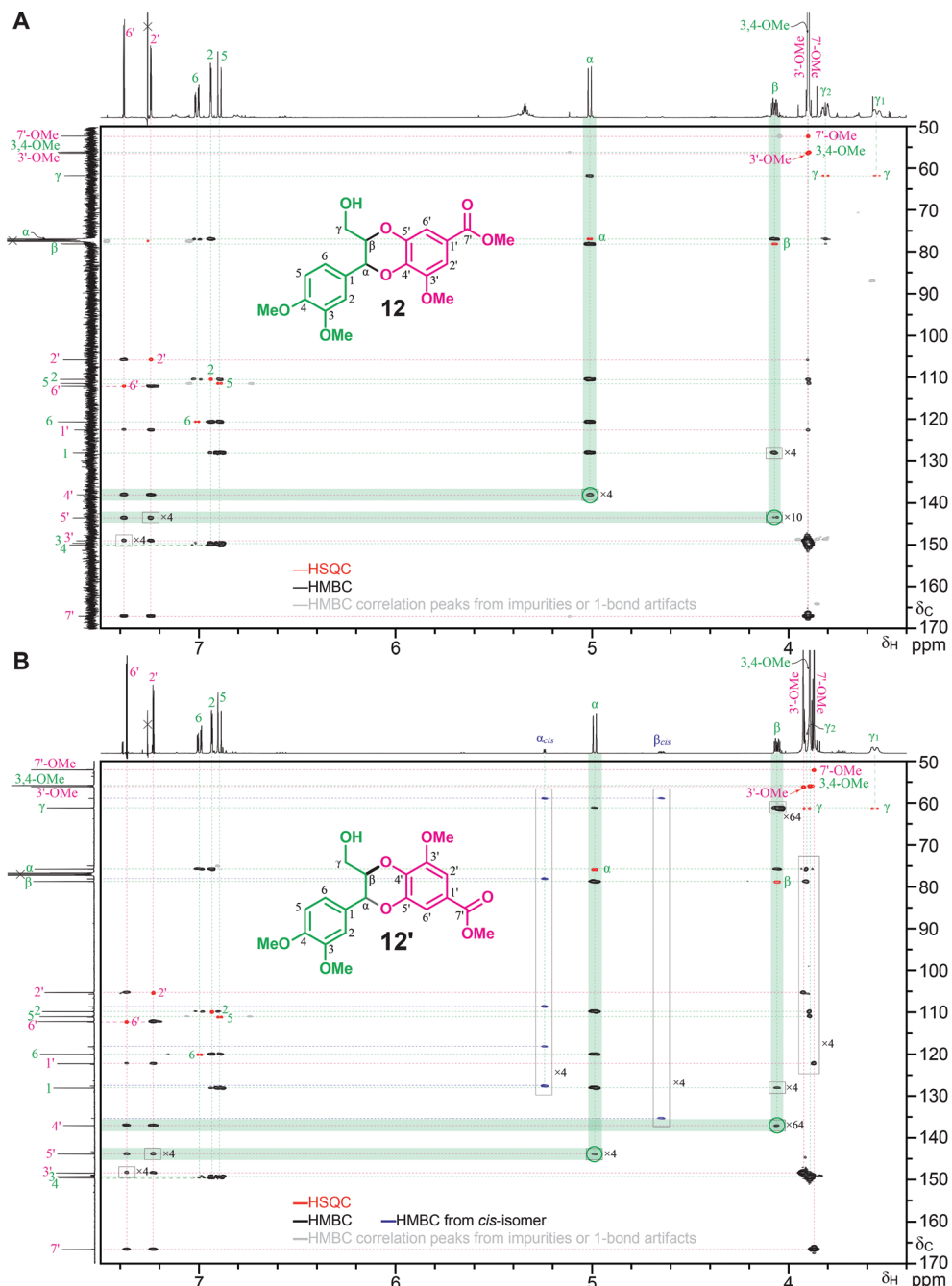


**Fig. 8**  $^1\text{H}$ - $^{13}\text{C}$  correlation spectra of the benzodioxane 12 from the Diels–Alder reaction between (A) 4-O-methylconiferyl alcohol 6 and the quinone 9 from methyl 5-hydroxyvanillate 11, and (B) of the benzodioxane 12' from the radical coupling reaction between coniferyl alcohol 1 and methyl 5-hydroxyvanillate 11 followed by simple phenolic methylation to produce the compound analogous to 12 and allow the determination that these are isomers and are not the same products. HSQC (red contours and assignments) spectra are overlaid (from separate spectrum/experiments). HMBC spectra (black correlations) show (with green highlighting) (A) correlations of proton  $\beta$  to carbon 5' and proton  $\alpha$  to carbon 4' that define the regiochemistry, and (B) correlations of proton  $\alpha$  to carbon 5' and proton  $\beta$  to carbon 4' that define its different regiochemistry. Some correlations required vertical expansion (by the factor indicated beside the box) to be seen on the current plot. Other correlations aid in assignments. Of major significance are the following points. (A) This benzodioxane 12 is the product of apparent  $\beta$ -O-5-coupling, but the mechanism is in fact [4+2]-cycloaddition. As shown by the green shading, proton  $\alpha$  correlates with six carbons:  $\gamma$ ,  $\beta$ , 2, 6, 1, and, importantly, 4' (in chemical shift order). Similarly, proton  $\beta$  correlates with three carbons:  $\alpha$ , 1, and, importantly, 5'. (B) The radical coupling benzodioxane 12' is the product of  $\beta$ -O-4-coupling, as is usual for coupling of a monolignol with a phenolic. As shown by the green shading, proton  $\alpha$  correlates with six carbons:  $\gamma$ ,  $\beta$ , 2, 6, 1, and, importantly, 5' (in chemical shift order). Similarly, proton  $\beta$  correlates with four carbons:  $\gamma$ ,  $\alpha$ , 1, and, importantly, 4', establishing the  $\beta$ -O-4-coupling. Note that the *cis*-isomer in the benzodioxane ring system, *cis*-12', is readily seen, in the 1D proton and carbon projections, and as highlighted for the proton  $\alpha$  and  $\beta$  correlations by the dark blue contours; the *cis*-ring isomer is typically seen at about the 5% level in such radical coupling products. For both A and B, contours colored light gray are from residual 1-bond correlations (split by the 1-bond  $^{13}\text{C}$ - $^1\text{H}$  coupling constant) from some peaks due to deviation from the set average value (145 Hz) or are from minor impurities.



(5H) units in the lignin of wild-type *Arabidopsis* plants remained below the detection limit, lignin of engineered lines contained up to ~70% 5H units. More recently, specialized C-lignins derived from 100% caffeyl alcohol,<sup>23–27</sup> or 5H-lignins from 100% 5-hydroxyconiferyl alcohol,<sup>24</sup> have been discovered. These lignins are the most likely to involve the production of quinones by oxidation/dehydrogenation and therefore have the most chance of being produced *via* Diels–Alder reactions. We don't have the exact models to provide comparative data for the products that would be expected in these lignins and predicting shifts from our model to the C- or 5H-lignin does not seem to be particularly reliable. The most diagnostic way for the oxatricyclo products (as in compounds **13** and **15**) is to look for the diagnostic set of nine HMBC correlations from proton  $\alpha$  (as in Fig. 5 and 7) along with the five correlations from proton  $\beta$ , but HMBC experiments, even on clean lignins, usually have only weak correlations at best for minor structures. The more sensitive way is to attempt to find the set of HSQC correlations consistent with these Diels–Alder structures (from the best predicted shifts). In searching through all of the NMR data from our publications on C- and 5H-lignins noted above, we could not find any convincing evidence for the presence of Diels–Alder products in any of them.

Can we leverage the observation that the benzodioxane regiochemistry is different to provide further evidence for radical coupling *vs* Diels–Alder mechanisms in lignification? Again, the HMBC approach is not very sensitive, and the  $\alpha$ - and  $\beta$ -H/C correlations are not so different that they would be expected to be well-separated in HSQC spectra, particularly when considering that the peaks in lignin spectra are significantly broader than in the models. Clearly, better spectra, and HMBCs are going to be necessary to seek benzodioxane regioisomers and the other diagnostic Diels–Alder products, or we need to look for such products by more sensitive methods, such as by HPLC-MS (although it is not obvious how to release them efficiently from the polymer; we suspect that hydrogenolysis may be the best way as it fully cleaves benzodioxane structures<sup>26</sup>), but so far we simply do not see any evidence for either. What is clearly evident is the presence of the *cis*-benzodioxane rings for C- and 5H-lignins,<sup>23–27</sup> as well as in piceanol lignins,<sup>28</sup> an observation again consistent with radical coupling but not Diels–Alder reactions.

We therefore have to accommodate the current lack of evidence for Diels–Alder coupling products produced between a hydroxycinnamyl alcohol, whether etherified or not, and an *o*-benzoquinone that might logically be produced from the catechyl units in such systems. This was particularly sobering after identifying Diels–Alder products in our model reactions, and the tantalizing prospect that it could reveal a new mechanism in lignification – a mechanism that would allow chain-extension at the phenolic and even at the non-phenolic ends of the lignin polymer chain. However, this absence of verifiable structures derived *via* Diels–Alder coupling in lignins has particularly important ramifications regarding lignification. First, lignification, the process of growing lignin polymer chains from hydroxycinnamyl alcohol (or other) monomers,

needs to be recognized even more strongly now as being constrained to, rather strictly, radical coupling reactions. Second, coupling is exclusively *via* the radical produced from oxidative 'radicalization' of the 4-OH (even if that may be in simple equilibrium with other phenolic radicals); only products from the 4-O radical are observed from the 3,4-dihydroxyphenyl monomers such as caffeyl alcohol and 5-hydroxyconiferyl alcohol. Third, after radical coupling, rearomatization can occur *via* internal trapping by the 3-OH for catechyl units and the 5-OH for 5-hydroxyguaiacyl units, whereby the benzodioxane rings are primarily *trans* (*E*) with minor *cis* (*Z*) ring-isomers. Additionally, although catechyl units might be expected to produce quinones under the oxidative (dehydrogenative) conditions present in the cell wall during lignification, all lignin units identified to date comport with single-electron oxidation processes and radical coupling and not from these two-electron-oxidized species and their possible [4+2]-cycloaddition (Diels–Alder) reactions.

The latter point, that quinones don't appear to be involved to any significant extent in lignification, is important because the conversion of catechols to quinones has at times been strongly advocated in the literature.<sup>33,34</sup> The notion that catechols are problematic for lignification has been mitigated by the repeated observations of lignins from such catechols in a range of viable natural, mutant, and transgenic plants, in which the monomers clearly incorporate into the polymer by the canonical radical coupling processes, as we have reviewed.<sup>3,4,12,35</sup> Here we find that quinones can form, at least from strongly conjugated species like methyl 5-hydroxyvanillate **11**, in simulated lignification processes (Fig. 3), from which they may react to produce dimers and higher oligomers. The lack of evidence for Diels–Alder and other quinone reactions complicating the polymer structure from a variety of lignins from plants utilizing high levels of catechyl monomers, however, suggests that processes other than radical coupling are at the very least minor. We remain open to the possibility that trace quantities of such Diels–Alder products may be detected in lignins at some point, but there is currently no evidence that cycloaddition reactions represent a significant pathway; small unassigned NMR  $^1\text{H}$ – $^{13}\text{C}$  correlation peaks in some lignins certainly remain to be elucidated. Additional evidence has come recently from the manner in which piceanol, a catechyl stilbene from outside the monolignol biosynthetic pathway, incorporates into lignins; again, the product array noted is entirely compatible with radical-coupling arguments.<sup>28–31,59,60</sup> A credible explanation for an absence of Diels–Alder products and mechanisms is likely premature, but it may be because of the exact nature of the substrates themselves, the caffeyl alcohol and the 5-hydroxyconiferyl alcohol that, even as quinones, are not as electron deficient as the methyl 5-hydroxyvanillate **11** examined here, or perhaps simply that radical coupling reactions simply out-compete the disproportionation reaction required to generate the quinone (for which two catechyl radicals need to encounter each other) in the cell wall. Regardless, and as evidence has already shown (above), catechols do undergo (one-electron oxidation and)



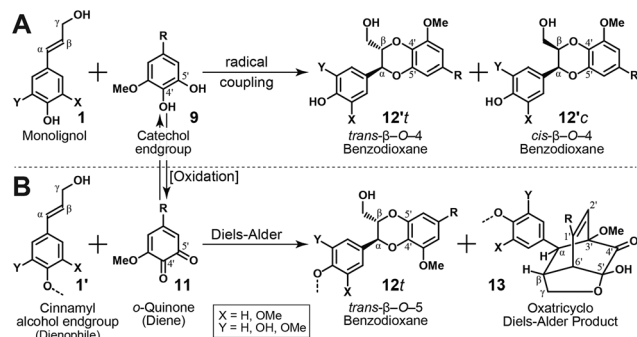


**Fig. 9** Summary of radical coupling vs *in vitro* Diels–Alder pathways and products. (A) Radical coupling of a monolignol with a general catechyl lignin end-unit; (B) Diels–Alder reaction of a general cinnamyl alcohol unit (usually on the starting end of a polymer chain) with a quinone. Note that the radical coupling pathway produces benzodioxanes **12'** from  $\beta$ -O-4 coupling, whereas the Diels–Alder coupling produces benzodioxanes **12** that would be described as  $\beta$ -O-5-coupled were they derived from radical coupling.

efficient radical coupling to produce either copolymeric or homopolymeric lignins.

## Conclusions

Two sets of reactions are shown here to operate if catechyl structures can be oxidized to their *o*-benzoquinones, (Fig. 3, and as summarized in Fig. 9). First, the quinone can oxidize a cinnamyl alcohol to a cinnamaldehyde, itself being reduced (back) to the catechol (Fig. 3). More importantly in the context of this paper, the quinone can function with either the 1,2-diketone or the conjugated diene as the diene component of a Diels–Alder reaction, with any cinnamyl alcohol unit, including those that are not free-phenolic, functioning as the dienophile (Fig. 9). At least with the components used here (Fig. 3), quinone **9** and dienophile **6**, the major Diels–Alder products were single isomers (although certainly as enantiomeric pairs) of the benzodioxane **12** and the oxatricyclo product **13** (Fig. 3). The key implication is that catechols such as caffeyl alcohol and 5-hydroxyconiferyl alcohol can first oxidize to *o*-quinones and subsequently may undergo either/both of two Diels–Alder reactions with general cinnamyl alcohols, including the monolignols, to potentially produce benzodioxane and oxatricyclo products. Importantly, a free-phenolic cinnamyl alcohol unit is not required, so the Diels–Alder mechanism would provide a way of extending the lignin polymer from the non-phenolic ‘starting end’ of a lignin chain, a pathway that is not typically possible *via* the usual radical-coupling pathways of lignification. As we can find no evidence of Diels–Alder products in natural lignins, even in lignins derived solely from catechyl monomers, we are forced to contend that they are not significant in the lignification of plants examined to date. As it stands, all product units seen in lignins of diverse types therefore comport with their being derived solely from radical coupling in single-electron oxidation processes. No further modifying

cation is therefore required at this point to the existing theory of lignification as a process of combinatorial radical coupling of phenols, with lignins deriving from a variety of phenolic monomers including the many examples now of non-canonical monomers.<sup>3,6,8,11–14,17,28–31,49,56,58–81</sup>

## Experimental

### Materials

*ortho*-Chloranil, methyl gallate, sodium borohydride were purchased from Acros Organics. Acetone, acetone-*d*<sub>6</sub>, chloroform-*d*, 3,4-dimethoxycinnamic acid, ethyl chloroformate, toluene, and THF were purchased from Sigma-Aldrich (St Louis, MO, USA).

### Methods

**QTOF-MS analysis.** Samples of the purified model compounds were dissolved in methanol (0.5 mg mL<sup>-1</sup>). Aliquots (1  $\mu$ L) from the sample solutions were subjected to chromatography on a Shimadzu Nexera X2 system (Kyoto, Japan) using Kinetex XB-C18 column (1.7  $\mu$ m, 50  $\times$  2.1 mm, 100A) (Phenomenex, Torrance, CA, USA) at 50 °C. The mobile phase consisted of 0.1% formic acid in H<sub>2</sub>O (A) and MeOH (B) at a flow rate of 0.6 mL min<sup>-1</sup>, in which the run was 5% B isocratically for 1 min, followed by linear gradient to 95% B at 4 min, isocratic with 95% B for 1 min; the column was returned to its initial conditions by using a linear gradient to 5% B at 6 min, and isocratic with 5% B for 2 min.

The mass spectra were acquired in the range of 50–1000 *m/z* units on a Bruker Daltonics quadrupole time-of-flight (QTOF) Impact II instrument (Bruker, Billerica, MA, USA), operating in negative-ion mode [ESI<sup>-</sup>]. The nebulizing gas pressure was set at 4 bar, the drying gas flow at 8 L min<sup>-1</sup>, the drying gas temperature was at 210 °C, and the capillary voltage was set at 3.50 kV. Sodium formate was used as a calibration standard.

**Nuclear magnetic resonance (NMR).** The products were dissolved in 0.6 mL of deuterated solvents (CDCl<sub>3</sub>, acetone-*d*<sub>6</sub>). NMR spectra were acquired on a Bruker Biospin AVANCE III 500 MHz spectrometer (Bruker Biospin, Bruker, Billerica, MA, USA) equipped with a cryogenically cooled 5 mm <sup>1</sup>H/<sup>13</sup>C-optimized triple resonance (<sup>1</sup>H/<sup>13</sup>C/<sup>15</sup>N) TCI gradient probe with inverse geometry (proton coils closest to the sample), or on a Bruker Neo 700 MHz spectrometer similarly equipped with a 5 mm QCI <sup>1</sup>H/<sup>31</sup>P/<sup>13</sup>C/<sup>15</sup>N cryoprobe. Bruker’s Topspin 4.1.3 software (MacOS) was used to process spectra; linear prediction was not used. Spectra were exported as pdf files and colorized in Adobe Illustrator; all spectra are resolution-independent vector figures that can be expanded without resolution-loss on screen to examine details. The central solvent peaks were used as internal reference ( $\delta_{\text{C}}/\delta_{\text{H}}$  CDCl<sub>3</sub> 77.0/7.26 ppm, acetone-*d*<sub>6</sub> 29.8/2.04 ppm). Standard Bruker pulse sequences were used for all spectra. The following parameters were used for the various 2D spectra in figures plotted here and in the ESI.†

COSY (homonuclear correlation spectroscopy) at 500 MHz: cosygpmfq pulse program, acquired from 10 to 0 ppm in F2 ( $^1\text{H}$ ) with 2k data points (acquisition time, 205 ms) and 10 to 0 ppm in F1 ( $^1\text{H}$ ) with 512 increments (F1 acquisition time, 102 ms) of 2 scans with a 1.5 s interscan delay, 30.5 min total acquisition time, processed to  $2\text{k} \times 1\text{k}$  using sine-squared apodization in each dimension.

NOESY (nuclear Overhauser effect spectroscopy) at 500 MHz: noesyph pulse program, acquired from 10 to 0 ppm in F2 ( $^1\text{H}$ ) with 2k data points (acquisition time, 205 ms) and 10 to 0 ppm in F1 ( $^1\text{H}$ ) with 256 increments (F1 acquisition time, 25.6 ms) of 8 scans with a NOESY mixing time of 300 ms, and a 2 s interscan delay, 1 h 26 min total acquisition time, processed to  $2\text{k} \times 1\text{k}$  using Gaussian apodization (GB = 0.001, LB = -0.1) in F2 and cosine-squared F1.

HSQC (Heteronuclear single-quantum coherence) for compounds **12** and **13** at 500 MHz: hsqcetgpsi2.2 pulse program, acquisition from 10 to 0 ppm in F2 ( $^1\text{H}$ ) with 2k data points (acquisition time, 200 ms) and 200 to 0 ppm in F1 ( $^{13}\text{C}$ ) with 400 increments (F1 acquisition time, 8 ms) of 2 scans with a 1 s interscan delay; the  $d_{24}$  delay was set to 0.89 ms (1/8J,  $J$  = 140 Hz) optimized for all multiplicities, 17 min total acquisition time, processed to  $2\text{k} \times 1\text{k}$  using Gaussian apodization (GB = 0.001, LB = -0.1) in F2 and cosine-squared in F1.

HSQC for compounds **12'** and **15** at 700 MHz: hsqcetgpsi2.2 pulse program, acquisition from 11.65 to -0.65 ppm in F2 ( $^1\text{H}$ ) with 3448 data points (acquisition time, 200 ms) and 215 to -5 ppm in F1 ( $^{13}\text{C}$ ) with 618 increments (F1 acquisition time, 8 ms) of 4 scans with a 1 s interscan delay, the  $d_{24}$  delay was set to 0.89 ms (1/8J,  $J$  = 140 Hz) optimized for all multiplicities, 51 min total acquisition time, processed to  $4\text{k} \times 1\text{k}$  using Gaussian apodization (GB = 0.001, LB = -0.1) in F2 and cosine-squared in F1.

HMBC (heteronuclear multiple-bond correlation) for compounds **12** and **13** at 500 MHz: hmbcglpndqf pulse program, acquisition from 10 to 0 ppm in F2 ( $^1\text{H}$ ) with 4k data points (acquisition time, 410 ms) and 200 to 0 ppm in F1 ( $^{13}\text{C}$ ) with 400 increments (F1 acquisition time, 16 ms) of 4 scans with a 1 s interscan delay, long-range  $J$ -coupling evolution time  $d_6$  of 80 ms ( $J_{\text{LR}}$  = 6.25 Hz), 40.5 min total acquisition time, processed to  $4\text{k} \times 1\text{k}$  using Gaussian apodization [GB = 0.195 (=  $d_6/\text{AQ}$ ), LB = -20)] in F2 and sine in F1.

HMBC for compounds **12'** and **15** at 700 MHz: hmbcglpndqf pulse program, 11.65 to -0.65 ppm in F2 ( $^1\text{H}$ ) with 4096 data points (acquisition time, 238 ms) and 215 to -5 ppm in F1 ( $^{13}\text{C}$ ) using non-linear sampling (NUS, 25%) with 1160 increments (F1 acquisition time, 30 ms) of 64 scans with a 1 s interscan delay, long-range  $J$ -coupling evolution time  $d_6$  of 80 ms ( $J_{\text{LR}}$  = 6.25 Hz), 5 h total acquisition time, NUS processed to  $4\text{k} \times 2\text{k}$  using Gaussian apodization [GB = 0.337 (=  $d_6/\text{AQ}$ ), LB = -10)] in F2 and sine in F1.

**Reaction of coniferyl alcohol with 4-O-methylconiferyl alcohol.** Coniferyl alcohol **1** (CA, 50 mg, 0.28 mmol), 4-O-methylconiferyl alcohol **6** (31 mg) and 3,4-dimethoxybenzaldehyde (as an internal standard (I.S.), 14 mg) were dissolved in

15 mL acetone (Fig. 1B and 2). To the mixture was added 85 mL sodium phosphate buffer (pH 5.0). A 10 mL aliquot of this mixture was removed for analysis of the starting mixture and extracted with EtOAc (10 mL, 2 $\times$ ). The combined EtOAc fractions were washed with saturated  $\text{NH}_4\text{Cl}$  solution, separated, dried over anhydrous  $\text{MgSO}_4$ , filtered, and the solvent evaporated under vacuum. Aliquots of this mixture were silylated and subjected to GC-MS.

The rest (90 mL) of the starting mixture was used for the typical peroxidase-mediated free-radical coupling reaction. Thus, 13 mg of urea- $\text{H}_2\text{O}_2$  was added while stirring, followed by adding 0.5 mg (dissolved in 1 mL water) of horseradish peroxidase (EC 1.11.1.7, 181 purpurogallin units per mg solid, type II, Sigma-Aldrich). The mixture was stirred for 20 min, and then was extracted with an equal volume of EtOAc (90 mL, 2 $\times$ ), the combined EtOAc solution was washed with saturated  $\text{NH}_4\text{Cl}$  solution and processed as above. About 6 mL of the EtOAc were evaporated using rotary evaporation under reduced pressure. The resulting product mixture was silylated using *N*, *O*-bis(trimethylsilyl)trifluoroacetamide (BSTFA) and subjected to GC-MS analysis.

GC conditions: injector temperature 250 °C; initial temperature 100 °C, hold for 1 min; ramp at 5 °C min $^{-1}$  to 180 °C, hold for 1 min; then ramp at 10 °C to 300 °C, and hold for 8 min. MS detector: ion source temperature 300 °C; EI mode. GC column: ZB-5HT, length 15 m; thickness 0.25 μm; diameter 0.25 mm.

**Preparation of dienophile 6.** The required non-phenolic cinnamyl alcohol **6** (4-O-methylconiferyl alcohol = 3,4-dimethoxy-cinnamyl alcohol) was prepared from its cinnamic acid analog *via* reduction of its carbonate derivative. 3,4-Dimethoxycinnamic acid (2.08 g, 10.0 mmol) was dissolved in THF (20 mL). Triethylamine (1.46 mL, 10.5 mmol) was added to the solution. The mixture was stirred at 0 °C for 10 min. Ethyl chloroformate (1.00 mL, 10.5 mmol) was slowly added over 10 min. After the reaction mixture was stirred for 15 min, the reaction mixture was filtered to remove the precipitated salt. The obtained filtrate was added into a cold  $\text{NaBH}_4$  (3.234 g, 85.5 mmol) suspension in THF/ $\text{H}_2\text{O}$  (v/v, 1/1). Then, the mixture was stirred at r.t. for 15 min. Aqueous  $\text{NH}_4\text{Cl}$  solution was added to the mixture to quench the borohydride and render the solution slightly acidic. The mixture was extracted with EtOAc, the obtained organic layer was washed with brine, dried with sodium sulfate, filtered, and the solvent evaporated *in vacuo* to obtain a crude oil. The crude oil was purified on a silica column (EtOAc : hexane = 1 : 2) to obtain 4-O-methylconiferyl alcohol **6** (1.639 g, 8.44 mmol). NMR (500 MHz,  $\text{CDCl}_3$ )  $\delta_{\text{H}}$ : 3.88 (s, 3H, 3-OMe), 3.90 (s, 3H, 4-OMe), 4.31 (d,  $J$  = 5.86 Hz, 2H,  $\gamma$ ), 6.25 (dt,  $J$  = 5.98, 15.79 Hz, 1H,  $\beta$ ), 6.55 (d,  $J$  = 15.86 Hz, 1H,  $\alpha$ ), 6.82 (d,  $J$  = 8.17 Hz, 1H, 5), 6.92 (dd,  $J$  = 1.90, 8.17 Hz, 1H, 6), 6.94 (d,  $J$  = 1.90 Hz, 1H, 2);  $\delta_{\text{C}}$ : 55.8 (OMe), 55.9 (OMe), 63.8 ( $\gamma$ ), 108.7 (2), 111.0 (5), 119.7 (6), 126.4 ( $\beta$ ), 129.6 (1), 131.1 ( $\alpha$ ), 148.8 (3), 148.9 (4).

**Preparation of diene/diketone 9.** Methyl 5-hydroxyvanillate **11** (methyl 3-O-methylgallate), prepared from methyl gallate as previously described,<sup>82</sup> was oxidized with *ortho*-chloranil to



obtain methyl 3-methoxy-1,2-dioxocyclohexa-3,5-diene-5-carboxylate **9**, the desired *o*-benzoquinone (Fig. 3).<sup>36</sup>

**Diels–Alder reaction of dimethoxycinnamyl alcohol **6** and *o*-benzoquinone **9**.** 4-O-Methylconiferyl alcohol **6** (19.6 mg, 0.101 mmol) was dissolved in acetone/toluene (v/v, 1/1), and the *o*-benzoquinone **9** (19.5 mg, 0.0994 mmol) was added. The reaction mixture was stirred at room temperature for 24 h, then concentrated *in vacuo* to obtain a crude oil. The obtained crude oil was separated *via* TLC to obtain the five main compounds: 4-O-methylconiferaldehyde **10** (7.27 mg, 0.0378 mmol, 32%), 4-O-methylconiferyl alcohol **6** (1.92 mg, 0.00989 mmol), methyl 5-hydroxyvanillate **11** (6.54 mg, 0.0330 mmol, 28%), a benzodioxane **12** (3.71 mg, 0.00950 mmol, 8%), and an oxatri-cyclo product **13** (14.77 mg, 0.0378 mmol, 32%), in which the approximate % conversion is noted in Fig. 3.

**Diels–Alder benzodioxane product *trans*-**12**.** NMR (500 MHz, CDCl<sub>3</sub>)  $\delta_{\text{H}}$ : 3.55 (bm, Hz, 1H,  $\gamma_1$ ), 3.81 (m, 1H,  $\gamma_2$ ), 3.897 (s, 3H, OMe), 3.899 (s, 3H, OMe), 3.902 (s, 3H, OMe), 3.904 (s, 3H, OMe), 4.07 (ddd,  $J$  = 8.15, 3.9, 2.8 Hz, 1H,  $\beta$ ), 5.01 (dd,  $J$  = 8.15 Hz, 1H,  $\alpha$ ), 6.90 (d,  $J$  = 8.25 Hz, 1H, 5), 6.94 (d,  $J$  = 2.0 Hz, 1H, 2), 7.01 (dd,  $J$  = 2.0, 8.25 Hz, 1H, 6), 7.24 (d,  $J$  = 1.9 Hz, 1H, 2'), 7.38 (d,  $J$  = 1.9 Hz, 1H, 6');  $\delta_{\text{C}}$ : 52.2 (7'-OMe), 55.9 (3'-OMe), 56.0 (3/4-OMe), 56.2 (4/3-OMe), 61.6 ( $\gamma$ ), 76.7 ( $\alpha$ ), 77.9 ( $\beta$ ), 105.5 (2'), 110.2 (2), 111.2 (5), 111.8 (6'), 120.4 (6), 122.3 (1'), 127.9 (1), 137.7 (4'), 143.2 (5'), 148.8 (3'), 149.3 (4\*), 149.8 (3\*), 166.7 (C=O); \* implies assignments may be reversed. LC-QTOF-MS:  $m/z$  [M – H]<sup>–</sup> calculated for C<sub>20</sub>H<sub>21</sub>O<sub>8</sub>: 389.1236; found: 389.1180.

**Diels–Alder product **13**.** NMR (500 MHz, CDCl<sub>3</sub>)  $\delta_{\text{H}}$ : 7.06 (dd,  $J$  = 1.13, 2.15 Hz, 1H, 2'), 6.77 (d,  $J$  = 8.20 Hz, 1H, 5), 6.58 (dd,  $J$  = 2.20, 8.20 Hz, 1H, 6), 6.56 (d,  $J$  = 2.20 Hz, 1H, 2), 4.38 (dd,  $J$  = 3.25, 8.30 Hz, 1H,  $\gamma_2$ ), 4.05 (dd,  $J$  = 2.15, 4.45 Hz, 1H, 6'), 4.02 (d,  $J$  = 8.30 Hz, 1H,  $\gamma_1$ ), 3.85 (s, 6H, 7'-OMe + 4-OMe), 3.81 (s, 3H, 3-OMe), 3.57 (s, 3H, 3'-OMe), 3.43 (t,  $J$  = 1.50 Hz, 1H,  $\alpha$ ), 2.85 (m,  $J$  = 1.6 Hz, 1H,  $\beta$ );  $\delta_{\text{C}}$ : 200.47 (4'), 163.89 (7'), 148.44 (3), 148.41 (4), 138.45 (2'), 132.25 (1'), 131.44 (1), 121.17 (6), 112.42 (2), 110.74 (5), 95.65 (5'), 86.78 (3'), 74.39 ( $\gamma$ ), 55.81 (4-OMe), 55.70 (3-OMe), 54.30 (3'-OMe), 52.56 (7'-OMe), 49.67 ( $\alpha$ ), 47.21 ( $\beta$ ), 44.90 (6'). LC-QTOF-MS:  $m/z$  [M – H]<sup>–</sup> calculated for C<sub>20</sub>H<sub>21</sub>O<sub>8</sub>: 389.1236; found: 389.1233.

**Benzodioxane **12'** from radical coupling followed by phenol-methylation.** Compound **12'a** was synthesized from the radical coupling of coniferyl alcohol **1** and methyl 5-hydroxyvanillate **11**, as detailed previously.<sup>42</sup> Methylation of **12'a** with iodomethane and K<sub>2</sub>CO<sub>3</sub> in acetone at room temperature for 16 h produced **12'** in almost quantitative yield; no purification was required.

**Benzodioxane product *trans*-**12'**.** NMR (500 MHz, CDCl<sub>3</sub>)  $\delta_{\text{H}}$ : 3.56 (bm, 1H,  $\gamma_1$ ), 3.87 (s, 3H, 7'-OMe), 3.89 (s, 6H, 3,4-OMe), 3.91 (bm, 1H,  $\gamma_2$ ), 3.93 (s, 3H, 3'-OMe), 4.06 (ddd, 1H,  $J$  = 2.6, 3.6, 8.2 Hz,  $\beta$ ), 4.99 (d,  $J$  = 8.2 Hz, 1H,  $\alpha$ ), 6.89 (d,  $J$  = 8.3 Hz, 1H, 5), 6.93 (d,  $J$  = 2.0 Hz, 1H, 2), 7.00 (dd,  $J$  = 2.0, 8.3 Hz, 1H, 6), 7.23 (d,  $J$  = 1.9 Hz, 1H, 2'), 7.37 (d,  $J$  = 1.9 Hz, 1H, 6');  $\delta_{\text{C}}$ : 52.1 (7'-OMe), 55.90 (3/4-OMe), 55.92 (4/3-OMe), 56.2 (3'-OMe), 61.3 ( $\gamma$ ), 75.9 ( $\alpha$ ), 78.8 ( $\beta$ ), 105.3 (2'), 109.9 (2), 111.1 (5), 112.2 (6'), 120.0 (6), 122.3 (1'), 128.1 (1), 137.1 (4'), 143.9 (5'), 148.4

(3'), 149.3 (3), 149.6 (4), 166.6 (7'). LC-QTOF-MS:  $m/z$  [M + Na]<sup>+</sup> calculated for C<sub>20</sub>H<sub>22</sub>O<sub>8</sub>Na<sup>+</sup>: 413.1207; found: 413.1168.

**Diels–Alder product **15** from a reaction between coniferyl alcohol **6** and methyl 5-hydroxyvanillate **11**.** Compound **15** was obtained following preparative-TLC separation from the same reaction that produced compound **12'a** above.

**Diels–Alder product **15**.** [There are two isomers (see Results and Discussion), so most peaks have two entries; for the <sup>13</sup>C NMR data, the two shifts are separated by a comma before the assignment; note that we use 3 significant figures only to show that the two peaks were resolved, and the difference between them]. NMR (700 MHz, acetone-d<sub>6</sub>)  $\delta_{\text{H}}$ : 7.59 (s, 0.5H, A4-OH), 7.58 (s, 0.5H, A4-OH), 7.03 (d,  $J$  = 2.20 Hz, 0.5H, A2), 7.02 (d,  $J$  = 2.20 Hz, 0.5H, A2), 6.95 (m, 0.5H, 2'), 6.94 (m, 0.5H, 2'), 6.87 (d,  $J$  = 8.10 Hz, 1H, A6), 6.80 (d,  $J$  = 8.10 Hz, 1H, A5), 6.72 (m, 0.5H, B6), 6.66 (m, 0.5H, B6), 6.62 (bd,  $J$  = 1.6 Hz, 1H, B2), 6.23 (s, 0.5H, 5'-OH), 6.22 (s, 0.5H, 5'-OH), 5.52 (d,  $J$  = 6.9 Hz, 0.5H, A $\alpha$ ), 5.51 (d,  $J$  = 6.9 Hz, 0.5H, A $\alpha$ ), 4.33 (dd,  $J$  = 3.5, 8.1 Hz, 0.5H, B $\gamma$ 2), 4.31 (dd,  $J$  = 3.5, 8.1 Hz, 0.5H, B $\gamma$ 2), 4.03 (d,  $J$  = 8.10 Hz, 0.5H, B $\gamma$ 1), 4.02 (d,  $J$  = 8.10 Hz, 0.5H, B $\gamma$ 1), 3.87 (m, 1H, 6'), 3.83 (m, 1H, A $\gamma$ 2), 3.815 (s, 1.5H, A3-OMe), 3.811 (s, 1.5H, A3-OMe), 3.809 (s, 1.5H, 7'-OMe), 3.788 (s, 1.5H, 7'-OMe), 3.785 (s, 3H, B3-OMe), 3.77 (m, 1H, A $\gamma$ 1), 3.549 (s, 1.5H, 3'-OMe), 3.547 (s, 1.5H, 3'-OMe), 3.546 (m, 0.5H, B $\alpha$ ), 3.538 (m, 0.5H, B $\alpha$ ), 3.489 (dd,  $J$  = 6.3, 6.5 Hz, 0.5H, A $\beta$ ), 3.486 (dd,  $J$  = 6.3, 6.5 Hz, 0.5H, A $\beta$ ), 2.87 (m, 1H, B $\beta$ );  $\delta_{\text{C}}$ : 201.20, 201.08 (4'), 164.72, 164.65 (7'), 148.35, 148.34 (A3), 148.29, 148.28 (B4), 147.27, 147.25 (A4), 144.43, 144.36 (B3), 139.49, 139.48 (2'), 134.36, 134.27 (A1), 134.07, 133.93 (B1), 133.51, 133.47 (1'); 129.86, 129.74 (B5), 119.53 (A6), 118.89, 118.81 (B6), 115.63 (A5), 114.95, 114.81 (B2), 110.45, 110.43 (A2), 97.43, 97.37 (5'), 88.49, 88.45 (A $\alpha$ ), 88.20, 88.10 (3'), 74.67, 74.59 (B $\gamma$ ), 64.77, 64.60 (A $\gamma$ ), 56.272, 56.265 (B3-OMe), 56.259, 56.251 (A3-OMe), 54.88, 54.80 (A $\beta$ ), 54.01, 53.92 (3'-OMe), 52.50, 52.49 (7'-OMe), 50.12, 50.11 (B $\alpha$ ), 48.45, 48.27 (B $\beta$ ), 47.01 (6'). LC/Q-TOF MS:  $m/z$  [M + Na]<sup>+</sup> calculated for C<sub>29</sub>H<sub>30</sub>O<sub>11</sub>Na<sup>+</sup>: 577.1680; found: 577.1609.

### Computational details

All calculations have been performed using Gaussian 16, Revision C.01. Optimizations were completed using the default criteria, with the M06-2X density functional method and the 6-311++G(d,p) basis set with the GD3 empirical dispersion correction. Frequency calculations were also performed to verify the identification of a minimum, as evidenced by the absence of imaginary frequencies and for the determination of thermal corrections for thermodynamic quantities.

### Author contributions

D. A., F. L., and J. R. originated the project on Diels–Alder reactions of *o*-benzoquinones; D. A. and F. L. performed the reactions, isolated and purified products and, with J. R., identified and structurally validated all products; R. V., W. B., T. J. E., J. R. and F. L. worked on clarifying misconceptions of significa-



tion; T. J. E. performed the molecular modeling and DFT calculations; Y. T., J. R., and H. K. reanalyzed NMR data of lignins from various prior studies seeking evidence for Diels–Alder products; D. A. produced the original draft manuscript and figures; J. R. finalized the text, produced final figures and ESI;† A. E. and H. K. provided structural analysis data; all authors edited the final manuscript.

## Conflicts of interest

There are no conflicts to declare.

## Acknowledgements

J. R., F. L., H. K., A. E., and the laboratory operation supporting D. A. were funded by the DOE Great Lakes Bioenergy Research Center (DOE BER Office of Science DE-SC0018409). D. A. was supported by JSPS Overseas Research Fellowships. Y. T. acknowledges support from JSPS KAKENHI (#JP20H03044). We thank Dr Steven Karlen for assistance with QTOF-MS analysis. W. B. and R. V. acknowledge support by SBO-FISCH through the ARBOREF project (grant no. 140894). For T. J. E., this work was also made possible in part by a grant of high-performance computing resources and technical support from the Alabama Supercomputer Authority.

## References

- 1 K. Freudenberg and A. C. Neish, *Constitution and Biosynthesis of Lignin*, Springer-Verlag, Berlin-Heidelberg-New York, 1968.
- 2 K. V. Sarkany and C. H. Ludwig, *Lignins: Occurrence, Formation, Structure and Reactions*, Wiley-Interscience, New York, 1971.
- 3 J. Ralph, K. Lundquist, G. Brunow, F. Lu, H. Kim, P. F. Schatz, J. M. Marita, R. D. Hatfield, S. A. Ralph, J. H. Christensen and W. Boerjan, *Phytochem. Rev.*, 2004, **3**, 29–60.
- 4 W. Boerjan, J. Ralph and M. Baucher, *Annu. Rev. Plant Biol.*, 2003, **54**, 519–546.
- 5 H. Önnerud, L. Zhang, G. Gellerstedt and G. Henriksson, *Plant Cell*, 2002, **14**, 1953–1962.
- 6 J. Ralph, M. Bunzel, J. M. Marita, R. D. Hatfield, F. Lu, H. Kim, P. F. Schatz, J. H. Grabber and H. Steinhart, *Phytochem. Rev.*, 2004, **3**, 79–96.
- 7 R. D. Hatfield, J. Ralph and J. H. Grabber, *Planta*, 2008, **228**, 919–928.
- 8 J. Ralph, *Phytochem. Rev.*, 2010, **9**, 65–83.
- 9 U. Takahama, *Physiol. Plant.*, 1995, **93**, 61–68.
- 10 S. Sasaki, T. Nishida, Y. Tsutsumi and R. Kondo, *FEBS Lett.*, 2004, **562**, 197–201.
- 11 R. Vanholme, K. Morreel, C. Darrah, P. Oyarce, J. H. Grabber, J. Ralph and W. Boerjan, *New Phytol.*, 2012, **196**, 978–1000.
- 12 J. Ralph, C. Lapierre and W. Boerjan, *Curr. Opin. Biotechnol.*, 2019, **56**, 240–249.
- 13 J. C. del Río, J. Rencoret, P. Prinsen, Á. T. Martínez, J. Ralph and A. Gutiérrez, *J. Agric. Food Chem.*, 2012, **60**, 5922–5935.
- 14 W. Lan, J. Rencoret, F. Lu, S. D. Karlen, B. G. Smith, P. J. Harris, J. C. del Río and J. Ralph, *Plant J.*, 2016, **88**, 1046–1057.
- 15 G. Brunow, O. Karlsson, K. Lundquist and J. Sipilä, *Wood Sci. Technol.*, 1993, **27**, 281–286.
- 16 J. Ralph, J. Peng, F. Lu, R. D. Hatfield and R. F. Helm, *J. Agric. Food Chem.*, 1999, **47**, 2991–2996.
- 17 J. Ralph, G. Brunow, P. J. Harris, R. A. Dixon, P. F. Schatz and W. Boerjan, in *Recent Advances in Polyphenol Research*, ed. F. Daayf, A. El Hadrami, L. Adam and G. M. Ballance, Wiley-Blackwell Publishing, Oxford, UK, 2008, vol. 1, ch. 2, pp. 36–66.
- 18 J. Ralph and L. L. Landucci, in *Lignin and Lignans; Advances in Chemistry*, ed. C. Heitner, D. R. Dimmel and J. A. Schmidt, CRC Press (Taylor & Francis Group), Boca Raton, FL, 2010, ch. 5, pp. 137–234, DOI: 10.1201/EBK1574444865.
- 19 Y. Matsushita, Y. Oyabu, D. Aoki and K. Fukushima, *R. Soc. Open Sci.*, 2019, **65**, 29, DOI: 10.1186/s10086-019-1809-1.
- 20 C. Lapierre, M. T. Tollier and B. Monties, *C. R. Acad. Sci., Ser. III*, 1988, **307**, 723–728.
- 21 Y. Barrière, J. Ralph, V. Méchin, S. Guillaumie, J. H. Grabber, O. Argillier, B. Chabbert and C. Lapierre, *C. R. Biol.*, 2004, **327**, 847–860.
- 22 J. M. Marita, W. Vermerris, J. Ralph and R. D. Hatfield, *J. Agric. Food Chem.*, 2003, **51**, 1313–1321.
- 23 F. Chen, Y. Tobimatsu, D. Havkin-Frenkel, R. A. Dixon and J. Ralph, *Proc. Natl. Acad. Sci. U. S. A.*, 2012, **109**, 1772–1777.
- 24 F. Chen, Y. Tobimatsu, L. Jackson, J. Nakashima, J. Ralph and R. A. Dixon, *Plant J.*, 2013, **73**, 201–211.
- 25 Y. Tobimatsu, F. Chen, J. Nakashima, L. Jackson, L. L. Escamilla-Treviño, R. A. Dixon and J. Ralph, *Plant Cell*, 2013, **25**, 2587–2600.
- 26 Y. Li, L. Shuai, H. Kim, A. H. Motagamwala, J. K. Mobley, F. Yue, Y. Tobimatsu, D. Havkin-Frenkel, F. Chen, R. A. Dixon, J. S. Luterbacher, J. A. Dumesic and J. Ralph, *Sci. Adv.*, 2018, **4**, eaau2968.
- 27 X. Wang, C. Zhuo, X. Xiao, X. Wang, M. L. Docampo-Palacios, F. Chen and R. A. Dixon, *Plant Cell*, 2020, **32**, 3825–3845.
- 28 J. C. del Río, J. Rencoret, A. Gutiérrez, H. Kim and J. Ralph, *Plant Physiol.*, 2017, **174**, 2072–2082.
- 29 J. Rencoret, H. Kim, A. B. Evaristo, A. Gutiérrez, J. Ralph and J. C. del Río, *J. Agric. Food Chem.*, 2018, **66**, 138–153.
- 30 J. Rencoret, D. Neiva, G. Marques, A. Gutiérrez, H. Kim, J. Gominho, H. Pereira, J. Ralph and J. C. del Río, *Plant Physiol.*, 2019, **180**, 1310–1321.
- 31 J. C. del Río, J. Rencoret, A. Gutiérrez, T. Elder, H. Kim and J. Ralph, *ACS Sustainable Chem. Eng.*, 2020, **8**, 4997–5012.



32 K. O. Eyong, V. Kuete and T. Efferth, in *Medicinal Plant Research in Africa*, 2013, ch. 10, pp. 351–391, DOI: 10.1016/b978-0-12-405927-6.00010-2.

33 A. M. Anterola and N. G. Lewis, *Phytochemistry*, 2002, **61**, 221–294.

34 L. B. Davin, M. Jourdes, A. M. Patten, K.-W. Kim, D. G. Vassao and N. G. Lewis, *Nat. Prod. Rep.*, 2008, **25**, 1015–1090.

35 R. Vanholme, B. Demedts, K. Morreel, J. Ralph and W. Boerjan, *Plant Physiol.*, 2010, **153**, 895–905.

36 K. S. Feldman, S. Quideau and H. M. Appel, *J. Org. Chem.*, 1996, **61**, 6656–6665.

37 P. A. Grieco, K. Yoshida and P. Garner, *J. Org. Chem.*, 1983, **48**, 3137–3139.

38 A. Sadler, V. V. Subrahmanyam and D. Ross, *Toxicol. Appl. Pharmacol.*, 1988, **93**, 62–71.

39 V. Nair and S. Kumar, *J. Chem. Soc., Chem. Commun.*, 1994, 1341–1342.

40 V. Nair, B. Mathew, K. V. Radhakrishnan and N. P. Rath, *Tetrahedron*, 1999, **55**, 11017–11026.

41 J. C. Wozniak, D. R. Dimmel and E. W. Malcolm, *J. Wood Chem. Technol.*, 1989, **9**, 513–534.

42 J. Ralph, C. Lapierre, F. Lu, J. M. Marita, G. Pilate, J. Van Doorsselaere, W. Boerjan and L. Jouanin, *J. Agric. Food Chem.*, 2001, **49**, 86–91.

43 J. M. Marita, J. Ralph, C. Lapierre, L. Jouanin and W. Boerjan, *J. Chem. Soc., Perkin Trans. 1*, 2001, 2939–2945.

44 J. Ralph, C. Lapierre, J. Marita, H. Kim, F. Lu, R. D. Hatfield, S. A. Ralph, C. Chapple, R. Franke, M. R. Hemm, J. Van Doorsselaere, R. R. Sederoff, D. M. O’Malley, J. T. Scott, J. J. MacKay, N. Yahiaoui, A.-M. Boudet, M. Pean, G. Pilate, L. Jouanin and W. Boerjan, *Phytochemistry*, 2001, **57**, 993–1003.

45 J. M. Marita, J. Ralph, R. D. Hatfield, D. Guo, F. Chen and R. A. Dixon, *Phytochemistry*, 2003, **62**, 53–65.

46 K. Morreel, J. Ralph, F. Lu, G. Goeminne, R. Busson, P. Herdewijn, J. L. Goeman, J. Van der Eycken, W. Boerjan and E. Messens, *Plant Physiol.*, 2004, **136**, 4023–4036.

47 F. Lu, J. M. Marita, C. Lapierre, L. Jouanin, K. Morreel, W. Boerjan and J. Ralph, *Plant Physiol.*, 2010, **153**, 569–579.

48 K. Morreel, H. Kim, F. Lu, O. Dima, T. Akiyama, R. Vanholme, C. Niculaes, G. Goeminne, D. Inzé, E. Messens, J. Ralph and W. Boerjan, *Anal. Chem.*, 2010, **82**, 8095–8105.

49 Y. Tobimatsu, S. Elumalai, J. H. Grabber, C. L. Davidson, X. Pan and J. Ralph, *ChemSusChem*, 2012, **5**, 676–686.

50 C. S. Chu, T. H. Lee, P. D. Rao, L. D. Song and C. C. Liao, *J. Org. Chem.*, 1999, **64**, 4111–4118.

51 G. J. Bodwell and Z. Pi, *Tetrahedron Lett.*, 1997, **38**, 309–312.

52 G. J. Bodwell, Z. Pi and I. R. Pottie, *Synlett*, 1999, 477–479.

53 R. Gao, F. Lu, G. Goeminne, K. Morreel, W. Boerjan and J. Ralph, *TBD*, 2021, unpublished.

54 L. Jouanin, T. Goujon, V. de Nadaï, M.-T. Martin, I. Mila, C. Vallet, B. Pollet, A. Yoshinaga, B. Chabbert, M. Petit-Conil and C. Lapierre, *Plant Physiol.*, 2000, **123**, 1363–1373.

55 B. A. Simmons, D. Loqué and J. Ralph, *Curr. Opin. Plant Biol.*, 2010, **13**, 313–320.

56 R. Vanholme, B. De Meester, J. Ralph and W. Boerjan, *Curr. Opin. Biotechnol.*, 2019, **56**, 230–239.

57 J.-K. Weng, H. Mo and C. Chapple, *Plant J.*, 2010, **64**, 898–911.

58 R. Vanholme, J. Ralph, T. Akiyama, F. Lu, J. Rencoret Pazo, J. Christensen, A. Rohde, K. Morreel, R. De Rycke, H. Kim, B. Van Reusel and W. Boerjan, *Plant J.*, 2010, **64**, 885–897.

59 T. Elder, J. C. del Río, J. Ralph, J. Rencoret, H. Kim and G. T. Beckham, *Phytochemistry*, 2019, **164**, 12–23.

60 J. C. del Río, J. Rencoret, A. Gutiérrez, W. Lan, H. Kim and J. Ralph, in *Recent Advances in Polyphenol Research*, ed. J. Reed, V. de Freitas and S. Quideau, Wiley-Blackwell, 2021, vol. 7, ch. 7, pp. 177–206.

61 J. Ralph, in *The Science and Lore of the Plant Cell Wall Biosynthesis, Structure and Function*, ed. T. Hayashi, Universal Publishers (BrownWalker Press), Boca Raton, FL, 2006, pp. 285–293.

62 R. Vanholme, K. Morreel, J. Ralph and W. Boerjan, *Curr. Opin. Plant Biol.*, 2008, **11**, 278–285.

63 J. H. Grabber, P. F. Schatz, H. Kim, F. Lu and J. Ralph, *BMC Plant Biol.*, 2010, **10**, 1–13.

64 J. H. Grabber, D. Ress and J. Ralph, *J. Agric. Food Chem.*, 2012, **60**, 5152–5160.

65 S. Elumalai, Y. Tobimatsu, J. H. Grabber, X. Pan and J. Ralph, *Biotechnol. Biofuels*, 2012, **5**, 1–13.

66 J. H. Grabber, N. Santoro, C. E. Foster, S. Elumalai, J. Ralph and X. Pan, *BioEnergy Res.*, 2015, **8**, 1391–1400.

67 W. Lan, K. Morreel, F. Lu, J. Rencoret, J. C. del Río, W. Voorend, W. Vermerris, W. Boerjan and J. Ralph, *Plant Physiol.*, 2016, **171**, 810–820.

68 W. Lan, F. Lu, M. Regner, Y. Zhu, J. Rencoret, S. A. Ralph, U. I. Zakai, K. Morreel, W. Boerjan and J. Ralph, *Plant Physiol.*, 2015, **167**, 1284–1295.

69 Y. Mottiar, R. Vanholme, W. Boerjan, J. Ralph and S. D. Mansfield, *Curr. Opin. Biotechnol.*, 2016, **37**, 190–200.

70 R. Rinaldi, R. Jastrzebshi, M. T. Clough, J. Ralph, M. Kennema, P. C. A. Bruijninx and B. M. Weckhuysen, *Angew. Chem., Int. Ed.*, 2016, **55**, 8164–8215.

71 N. B. Eloy, W. Voorend, W. Lan, M. de Lyra Soriano Saleme, I. Cesarino, R. Vanholme, R. A. Smith, G. Goeminne, A. Pallidis, K. Morreel, J. Nicomedes Jr., J. Ralph and W. Boerjan, *Plant Physiol.*, 2017, **173**, 998–1016.

72 W. Lan, F. Yue, J. Rencoret, J. C. del Río, W. Boerjan, F. Lu and J. Ralph, *Polymers*, 2018, **10**, 916.

73 J. C. del Río, J. Rencoret, A. Gutierrez, H. Kim and J. Ralph, *J. Agric. Food Chem.*, 2018, **66**, 4402–4413.

74 P. Y. Lam, Y. Tobimatsu, N. Matsumoto, S. Suzuki, W. Lan, Y. Takeda, M. Yamamura, M. Sakamoto, J. Ralph, C. Lo and T. Umezawa, *Nat. Sci. Rep.*, 2019, **9**, 11597.

75 P. Y. Lam, A. C. Lui, M. Yamamura, L. Wang, Y. Takeda, S. Suzuki, H. Liu, F. Y. Zhu, M. X. Chen, J. Zhang, T. Umezawa, Y. Tobimatsu and C. Lo, *New Phytol.*, 2019, **223**, 204–219.



76 W. Lan, J. Rencoret, J. C. del Río and J. Ralph, in *Lignin: Biosynthesis, Functions, and Economic Significance*, ed. F. Lu and F. Yue, Nova Science Publisher, Inc., Hauppauge, NY, USA, 2019, ch. 3, pp. 51–78.

77 J. H. Grabber, C. L. Davidson, Y. Tobimatsu, H. Kim, F. Lu, Y. Zhu, M. Opietnik, N. Santoro, C. E. Foster, F. Yue, D. Ress, X. Pan and J. Ralph, *Plant Sci.*, 2019, **287**, 110070.

78 P. Oyarce, B. De Meester, F. Fonseca, L. de Vries, G. Goeminne, A. Pallidis, R. De Rycke, Y. Tsuji, Y. Li, S. Van den Bosch, B. Sels, J. Ralph, R. Vanholme and W. Boerjan, *Nat. Plants*, 2019, **5**, 225–237.

79 A. C. W. Lui, P. Y. Lam, K. H. Chan, L. Wang, Y. Tobimatsu and C. Lo, *New Phytol.*, 2020, **228**, 269–284.

80 T. Elder, J. C. del Río, J. Ralph, J. Rencoret, H. Kim, G. T. Beckham and M. F. Crowley, *ACS Sustainable Chem. Eng.*, 2020, **8**, 11033–11045.

81 T. Elder, J. Rencoret, J. C. del Río, H. Kim and J. Ralph, *Front. Plant Sci.*, 2021, **12**, 642848.

82 R. R. Scheline, *Acta Chem. Scand.*, 1966, **20**, 1182.

